
# BRNO UNIVERSITY OF TECHNOLOGY

VYSOKÉ UČENÍ TECHNICKÉ V BRNĚ

## FACULTY OF MECHANICAL ENGINEERING

FAKULTA STROJNÍHO INŽENÝRSTVÍ

## INSTITUTE OF AEROSPACE ENGINEERING

LETECKÝ ÚSTAV


# QUALIFICATION THERMO-VACUUM TESTS - VERIFICATION OF READINESS USING A DUMMY

PŘÍPRAVA KVALIFIKAČNÍCH TERMO-VAKUOVÝCH ZKOUŠEK KOSMICKÝCH ZAŘÍZENÍ

MASTER'S THESIS

DIPLOMOVÁ PRÁCE


AUTHOR — Bc. Samuel Kosír

AUTOR PRÁCE

SUPERVISOR — Ing. Jakub Mašek, Ph.D.

VEDOUCÍ PRÁCE



BRNO 2025

BRNO UNIVERSITY OF TECHNOLOGY
FACULTY OF MECHANICAL ENGINEERING

# Assignment Master's Thesis

| | |
|---|---|
| Institut: | Institute of Aerospace Engineering |
| Student: | **Bc. Samuel Kosír** |
| Degree programm: | Aerospace Technology Aircraft |
| Branch: | Design |
| Supervisor: | **Ing. Jakub Mašek, Ph.D.** |
| Academic year: | 2024/25 |

As provided for by the Act No. 111/98 Coll. on higher education institutions and the BUT Study and Examination Regulations, the director of the Institute hereby assigns the following topic of Master's Thesis:

## Qualification thermo–vacuum tests – verification of readiness using a dummy

**Brief Description:**

The design of devices for heat transfer in a vacuum environment shall to be verified in simulated laboratory conditions. The advantage of using a thermo–vacuum chamber is a wide range of measured temperatures and reduction of heat losses. The accuracy of the experimental measurement of the thermal conductivity thus depends on the instrumentation and phenomena such as thermal contact resistance.

**Master's Thesis goals:**

– Compile the test plan, measurement conditions and device configuration;
– Prepare the procedures of measurement and data evaluation;
– Experimental verification of qualification tests on a dummy sample.

**Recommended bibliography:**

ROTH, A. Vacuum technology. 3rd, updated and enlarged edition. North-Holland, 2012. ISBN 0-444-88010-0.

MAŠEK, Jakub. Qualification Test of Heat Switch for Martian Conditions. Master´s thesis, supervisor Ing. Robert Popela, Ph.D. Brno, 2016.

Deadline for submission Master's Thesis is given by the Schedule of the Academic year 2024/25

In Brno,

L. S.

| | |
|---|---|
| doc. Ing. Jaroslav Juračka, Ph.D.<br>Director of the Institute | doc. Ing. Jiří Hlinka, Ph.D.<br>FME dean |

# ABSTRACT

This thesis focuses on the development and validation of experimental procedures for thermal vacuum chamber (TVAC) testing of miniaturized heat switch (MHS) under space-relevant conditions. The main objective was to prepare the test setup, data evaluation procedure and methodology for future calibration and qualification of the TVAC facility. A series of pilot tests, cyclic tests, and thermal balance tests were conducted with bronze and aluminium dummies.

Cyclic testing in high vacuum and low-pressure $CO_2$ atmospheres validated the system's ability to achieve required temperature profiles and simulating orbital thermal cycling. Thermal balance tests were designed to quantify thermal parameters for copper-aluminium interfaces under steady-state conditions. Whilst successful in generating usable data, deviations in measured thermal resistance suggested sensitivity to mechanical setup, sensor positioning, and environmental conditions.

A thermal model was applied to analyze data and validate measured results. Observed issues, such as cable damage during cyclic testing and thermal contact resistance variation, informed recommendations for test stack design improvement and measurement consistency.

The thesis concludes by proposing further testing with an aluminium-aluminium interface to isolate material-specific behavior. The methods and insights developed here establish a foundation for future space component qualification and thermal system calibration.



**Key Words:** thermal vacuum chamber (TVAC), miniaturized heat switch (MHS), thermal contact resistance (TCR), thermal interface material, space simulation testing, steady-state measurement, aluminium dummy, heat flux, environmental testing of aerospace components, thermal model validation

# ABSTRAKT

Tato diplomová práce je zaměřena na vývoj a ověření experimentálních postupů pro testování miniaturního tepelného spínače (MHS) v termo-vakuové komoře (TVAC) za podmínek odpovídajících kosmickému prostředí. Hlavním cílem bylo připravit zkušební sestavu, postup vyhodnocení dat a metodiku pro budoucí kalibraci a kvalifikaci termo-vakuové komory. Byla provedena řada úvodních zkoušek, cyklických zkoušek a testů tepelné rovnováhy se vzorky z bronzu a hliníku.

Cyklické testy, které byly provedeny ve vysokém vakuu a $CO_2$ atmosféře potvrdili schopnost systému dosáhnout požadovaných teplotních profilů a simulovat tepelnou zátěž komponent na orbitě. Testy tepelné rovnováhy byly navrženy k určení tepelných veličin pro rozhraní měď-hliník v ustáleném stavu. I když se podařilo získat použitelná data, odchylky v naměřeném tepelném odporu naznačovaly citlivost na mechanické uspořádání komory, polohu senzorů a okolní podmínky.

Pro analýzu dat a validaci naměřených výsledků byl použit tepelný model. Zjištěné problémy, jako jsou poškození kabelů při cyklických testech a kolísání kontaktního tepelného odporu, podnítili ke vzniku doporučení pro zlepšení designu testovací sestavy a konzistenci měření.

Práce je zakončená návrhem dalších zkoušek pro rozhraní hliník-hliník pro izolaci materiálově specifického chování. Vyvinuté metody a poznatky jsou základem pro budoucí kvalifikaci vesmírných komponent a kalibraci tepelných systémů.

**Klíčová slova:** termo-vakuová komora (TVAC), miniaturní tepelný spínač (MHS), kontaktní tepelný odpor (TCR), materiál pro tepelné rozhraní, zkoušky simulující podmínky ve vesmíru, zkoušky v ustáleném stavu, hliníkový vzorek, tepelný tok, environmentální zkoušky komponent pro kosmické aplikace, validace tepelného modelu

# BIBLIOGRAPHY

KOSÍR, Samuel. *Qualification thermo-vacuum tests - verification of readiness using a dummy*. Master's Thesis. Jakub MAŠEK (supervisor). Brno: Brno University of Technology, Faculty of Mechanical Engineering, 2025.

## DECLARATION OF AUTHENTICITY

I declare that this thesis, entitled, “Qualification thermo-vacuum tests - verification of readiness using a dummy” is my original work and that all the sources that I have used or quoted have been listed at the end of this thesis.

In Brno on 23.5.2025

.....

Samuel Kosír

## ACKNOWLEDGEMENT

I would like to thank my thesis supervisor Ing. Jakub Mašek, Ph.D. for his support, valuable guidance, and constructive feedback throughout the course of this thesis. I would also like to thank my family for their continuous support, patience, and understanding during my studies. Their encouragement has been a constant source of strength and motivation.

# Table of Contents

# Introduction

Evolution in space technology has increased the demand for compact, efficient, and reliable thermal control systems with the capacity for operation in extreme environmental conditions. Among such technologies are miniaturized heat switches (MHS), that are critical to regulating heat transfer between spacecraft subsystems, especially in passive thermal control subsystems. Such components must operate effectively under high/ultra-high vacuum, substantial temperature cycling, and highly fluctuating thermal loads – difficult to simulate and evaluate conditions without precise ground-based test facilities.

To guarantee that components such as the MHS perform in space as intended, comprehensive ground testing in thermally controlled vacuum settings is essential. This is achieved by replicating the conditions of temperature and pressure in orbit, typically by the application of thermal vacuum chambers (TVAC).

The objective of this thesis is to enable future qualification and calibration of the existing thermal vacuum chamber to accommodate MHS-type component testing. This entails creating stable and repeatable test procedures, validation of data acquisition methods, and thermal measurement stability under cyclic and steady-state conditions. In particular, the focus is on developing the test environment and evaluation procedure to facilitate effective and repeatable thermal parameters measurement on test specimens.

To achieve this, this thesis builds upon the previous development of the thermal vacuum testing project at Institute of Aerospace Engineering, Brno University of Technology (IAE, BUT). Initial pilot tests were carried out, both in $CO_2$ and vacuum environments to refine the test methodology. New cyclic and thermal balance tests were also carried out, with the experiments being performed on specimens made from different materials, to further explore system sensitivity to material interfaces and to variation in the environment. A thermal model – originally developed in previous thesis – was modified and utilized to assist in experimental data interpretation and increase test setup confidence.

This thesis begins with theoretical foundation that applies to vacuum, heat transfer mechanisms, and space test requirements. It then describes the current state of thermal vacuum chamber and test procedures, followed by detailed breakdown of the tests conducted, results, and interpretation. The discussion assesses the implications of findings for future calibration activities and qualification campaigns of the miniaturized heat switch.

# 1 Theoretical Background

## 1.1 Vacuum

A vacuum is an empty space or a space without matter (from Latin word *vacuum*, meaning "void" or "vacant"). When considering a vacuum from a practical standpoint, it is a space where the gas pressure is significantly lower compared to the standard atmospheric pressure (=$1.013 \cdot 10^5$ Pa or 1013 mbar). In physical terms, it is a space where the number of gas molecules per unit of volume is substantially reduced, typically to the degree that molecular collisions are comparatively rare or almost non-existent. According to the American Vacuum Society, the density of molecules in space to be considered a vacuum, is less than $2.5 \cdot 10^{19}$ molecules/cm$^3$. A perfect vacuum (with zero particles) cannot be achieved [1].

Vacuum is usually expressed in terms of absolute pressure, that is measured in pascals [Pa], millibar [mbar] or torr [Torr]. As can be seen in Figure 1.1, the vacuum ranges are [1]:

(Note: $1\ Torr = 133.322\ Pa$)

- Low vacuum (from atm. pressure to about $10^{-2}$ Torr) – this range of vacuum can be achieved by using mechanical pumps (e.g., rotary vane or diaphragm pumps)
- Medium vacuum (1 to $10^{-3}$ Torr) – requires two-stage pumping system
- High vacuum ($10^{-3}$ to $10^{-7}$ Torr) – typically achieved with turbomolecular pumps
- Ultra-high vacuum (<$10^{-7}$ Torr) – requires extensive outgassing treatment and ion or cryopumps [2]

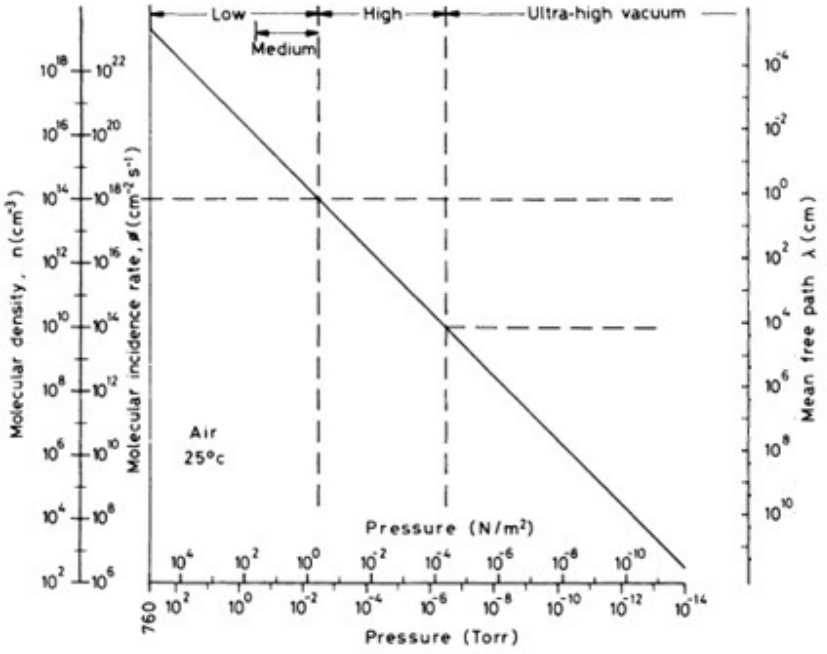


*Figure 1.1 Vacuum ranges [1]*

These categories are associated with the mean free path λ of gas molecules, which is the average distance a molecule in a gas travels between two consecutive collisions with other gas molecules. The mean free path is given by [2]:

$$\lambda = \frac{k_B T}{\sqrt{2}\pi d^2 p} \tag{1.1}$$

Where:

- $\lambda$ – mean free path [m]
- $k_B$ – Boltzmann constant (=$1.38 \cdot 10^{-23}$ J/K)
- T – temperature [K]
- d – effective molecular diameter [m]
- p – pressure [Pa]

The vacuum in space can be seen in Figure 1.2. Atmospheric pressure decreases with altitude as a result of the thinning of the atmosphere. Every 15 km the pressure drops by a factor of 10 up to 100 km altitude, that results in a pressure of $10^{-3}$ Torr at about 90 km. At these altitudes, high vacuum can be considered. In the ionosphere (100-400 km) the pressure decreases by a factor of 10 only every 100-200 km. The result is a pressure of $10^{-10}$ Torr at an altitude of 1000 km. Above 400 km, ultra-high vacuum conditions exist [1].

At orbital altitudes, pressure is more a function of spacecraft velocity and ambient gas density than static pressure itself. High-altitude atmospheric models are therefore often expressed in terms of molecular concentrations. Below 200 km the atmosphere is primarily air, in range of 200-1000 km, the atmosphere consists mostly of atomic nitrogen and oxygen (with increased ionization during solar maxima). The gas above altitude of 1500 km consists of protons, electrons and neutral atomic hydrogen [1].

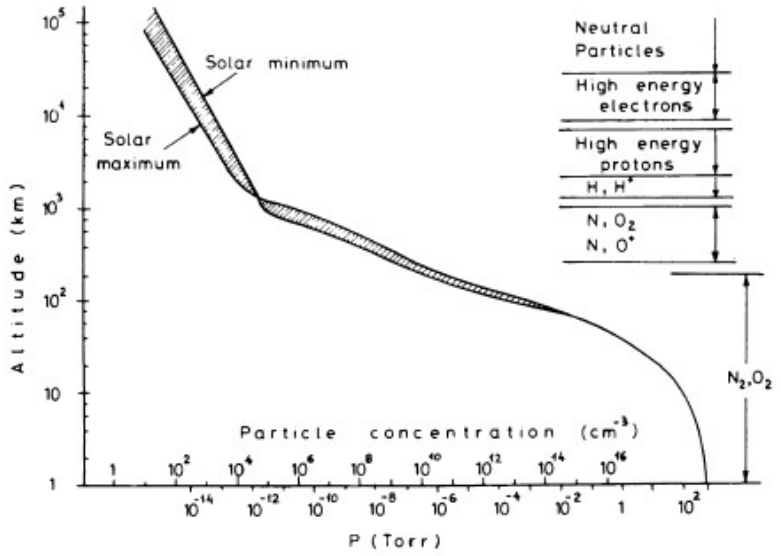


*Figure 1.2 Vacuum in space [1]*

## 1.2 Heat Transfer

Heat transfer is a physical process by which the thermal energy (heat) is moved from one region to another due to a temperature difference. In vacuum conditions, such as in space or thermal vacuum chamber, it is important to understand the dominating heat transfer mechanism for accurate experimental analysis. Heat can be transferred in three different modes: conduction, convection, and radiation, which respond differently in rarefied environments and are influenced by interaction of molecules, surface properties, and interface resistances.

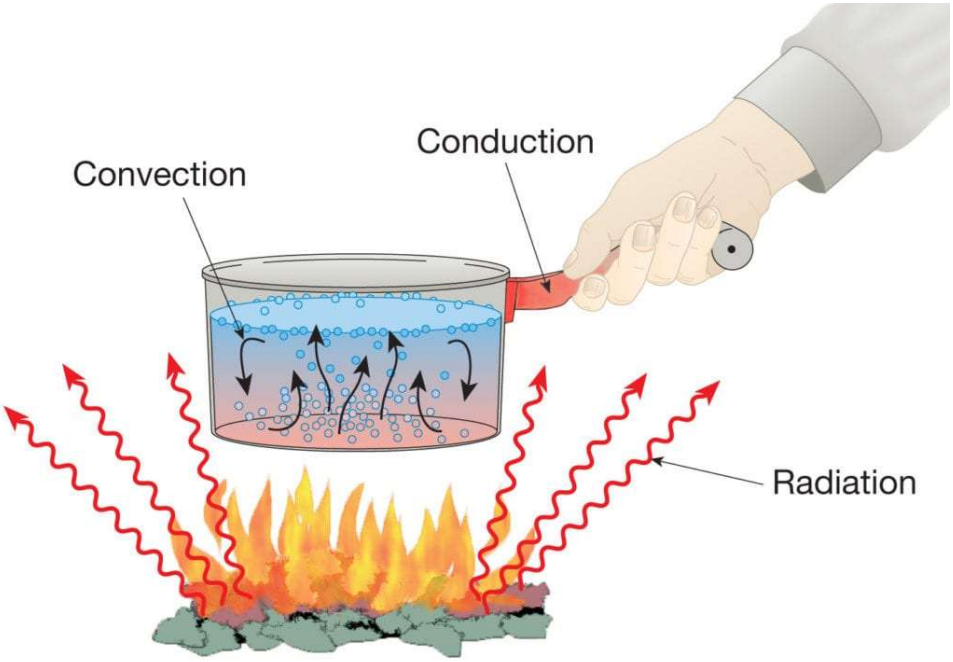


*Figure 1.3 Heat transfer mechanisms [3]*

**Knudsen Number and Regime Classification**

The Knudsen number (Kn) is a dimensionless parameter that characterizes the regime of gas behavior. It is defined as the ratio of the mean free path λ (described in Chapter 1.1) and a characteristic length scale L [m] [2]:

$$Kn = \frac{\lambda}{L} \tag{1.2}$$

Based on Knudsen number, different regimes of thermal transport apply [2]:

- $\mathrm{Kn} < 0.01$: Continuum regime – conventional conduction and convection dominate
- $0.01 < \mathrm{Kn} < 0.1$: Slip flow regime
- $0.1 < \mathrm{Kn} < 10$: Transitional flow
- $\mathrm{Kn} > 10$: Free molecular regime – convection is negligible, and radiation/conduction through solids dominates

This classification is important when interpreting heat transfer in thermal vacuum tests and space conditions, where the behavior of rarefied gas prevails.

**Thermal Conduction**

Conduction is the dominant method of heat transfer in solids and occurs due to molecular interactions with no bulk motion of matter. For one-dimensional isotropic materials it is described by Fourier's law [4]:

$$q_x = -k\frac{dT}{dx} \tag{1.3}$$

Where:

- $q_x$ – is the heat flux (in this thesis also written as HF) [W/m$^2$]
- k – is the thermal conductivity [W/m·K]
- $\frac{dT}{dx}$ – is temperature gradient
  (Note: The minus sign is a result, that heat is transferred in the direction of decreasing temperature.)

Under the steady-state conditions (Figure 1.4), the Fourier's law can be expressed as [4]:

$$q_x = k\frac{\Delta T}{L} \tag{1.4}$$

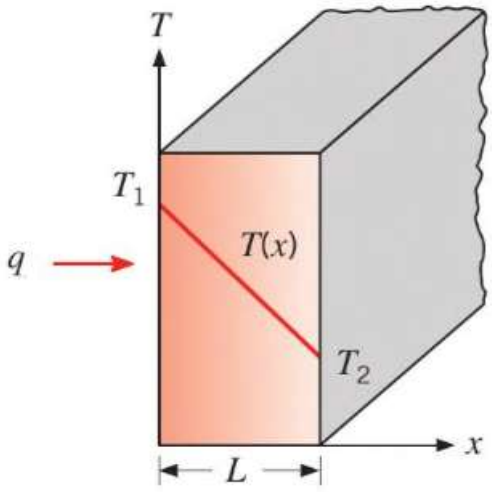


*Figure 1.4 One-dimensional thermal conduction [4]*

**Thermal-Electrical Analogy**

Heat conduction systems can be examined using the thermal-electrical analogy, which utilizes similar principles to those in electrical circuits. In this analogy:

- Temperature difference (ΔT) acts as a voltage (V)
- Heat transfer rate (Q) acts like current (I)
- Thermal resistance ($R_{th}$) acts as an electrical resistance (R)

Using this analogy, the Equation (1.4) can be interpreted as heat current flowing through a series of thermal resistors, where the total resistance is [4]:

$$R_{th,tot} = \sum_i \frac{L_i}{k_i A} \tag{1.5}$$

Where:

- $L_i$ is the thickness of each layer
- $k_i$ is the thermal conductivity of each layer
- A is the cross-sectional area

And the total heat flow is [4]:

$$Q = \frac{\Delta T}{R_{th,tot}} \tag{1.6}$$

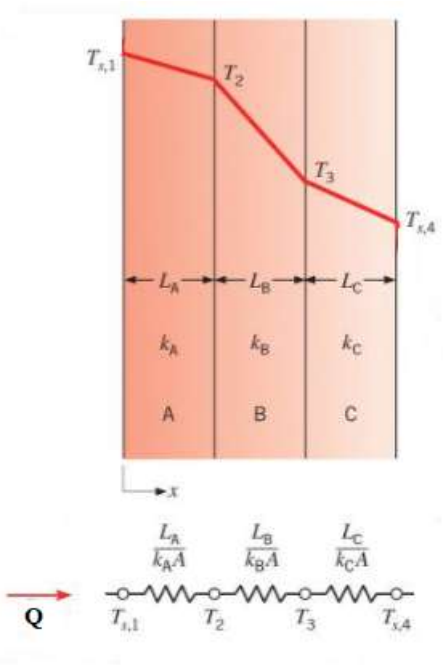


*Figure 1.5 Thermal-electrical Analogy [4]*

This modeling technique shown in Figure 1.5 is especially useful when analyzing temperature drops across layers or interfaces in stacked assemblies.

On closer inspection of the temperature profile (Figure 1.6), a temperature drop at plane 2 (the contact plane between two materials) can be seen. This is a result of thermal contact resistance (TCR).

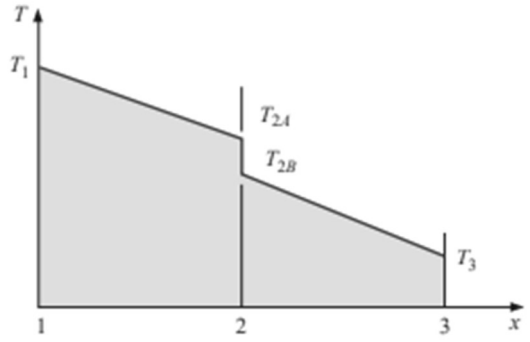


*Figure 1.6 Detailed temperature profile [5]*

The main cause of thermal contact resistance is the surface roughness effects (Figure 1.7). Between contact points are gaps, filled with air. Therefore, conduction across the actual area and conduction and/or radiation across the gaps are the causes of heat transfer. The contact resistance can be interpreted as two parallel resistances: the gap resistance and the contact point resistance. Usually, the contact area is small, and the gaps contribute significantly to the resistance, particularly for rough surfaces. Increasing the area of the contact spots, by reducing their roughness or increasing the joint pressure, can lower the contact resistance. The thermal contact resistance is defined as [4]:

$$TCR = \frac{T_A - T_B}{q_x} \tag{1.7}$$

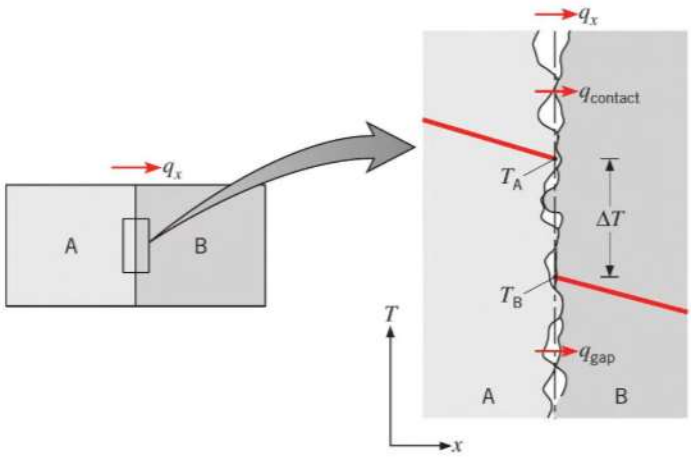


*Figure 1.7 Roughness model for analysis of TCR [4]*

**Convection**

Convection is the transfer of heat by movement of fluids (liquids or gases) (Figure 1.8). The basic relationship for convective heat transfer, defined by Newton's law of cooling is [5]:

$$q = hA(T_w - T_\infty) \tag{1.8}$$

Where:

- h is the convection heat-transfer coefficient [W/m$^2$·K]
- A is the surface area exposed to fluid [m$^2$]
- ($T_w - T_\infty$) is temperature difference between the wall and fluid [K]

Because of the large mean free path $\lambda$ of gas molecules in high vacuum environments, the convection is insignificant [2]. Therefore, in TVAC testing, convection is usually ignored or considered only as a low-vacuum case correction.

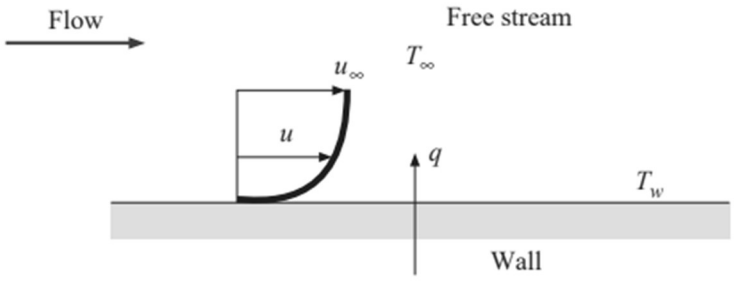


*Figure 1.8 Convection heat transfer [5]*

**Radiation**

Thermal radiation is energy emitted by all objects with temperatures above absolute zero, thanks to the movement of atoms and molecules. The energy of the radiation field is transferred by electromagnetic waves. In contrast to conduction or convection, radiation does not require the presence of a material medium, and heat can be transported in vacuum. As a matter of fact, heat transfer by radiation is most efficient in vacuum. The thermal radiation between two surfaces (Figure 1.9) can be described by Stefan-Boltzmann law [4], [5]:

$$q = \varepsilon\sigma A(T_1^4 - T_2^4) \tag{1.9}$$

Where:

- ε is the surface emissivity [-]
- σ is Stefan-Boltzmann constant (=5.67·10$^{-8}$ W/m$^2$K$^4$)
- A is radiating surface area [m2]
- $T_1, T_2$ are absolute temperatures of the two surfaces [K]

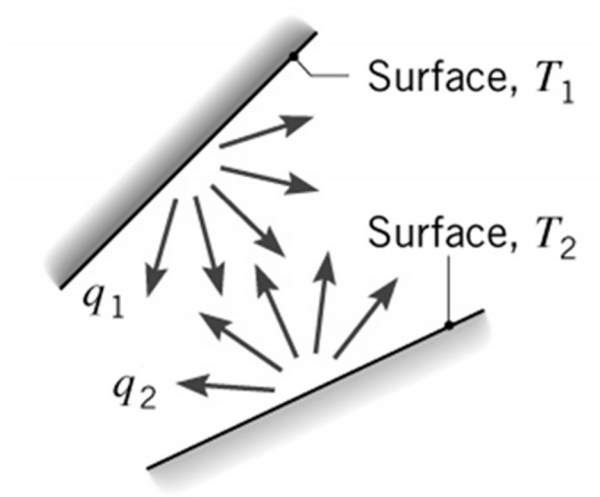


*Figure 1.9 Radiation heat exchange between two surfaces [6]*

## 1.3 Fundamentals of Steady State in Thermal Systems

The thermal steady state is a condition in which the temperature at each point inside a system remains constant over time. This implies that the rate of heat input in each region is exactly equal to the rate of heat output, without any net energy being stored within the material. That is, the temperature field is not time-dependent, and all the thermal gradients are spatially driven and temporally stable [4].

For one-dimensional conduction in solids, a steady state is necessary for the application of simplified heat transfer models such as Fourier's law (mentioned in previous chapter), where the heat flux is related to the temperature gradient and thermal conductivity. In the steady state, the thermal system can be modeled upon the basis that all transient thermal effects have been subsided and that the measured temperature gradient represents pure conductive heat transfer [4] [7].

In experimental settings, achieving steady state is very important for accurate measurement of thermal resistance, conductance or other evaluated thermal properties. This often involves stable boundary conditions, minimized external interference, and sufficient time for the system to reach thermal balance.

## 1.4 Vacuum Chamber Testing for Space Applications

Components that are designed for space operation must endure rigorous environmental qualification in simulated conditions of orbital environment to ensure performance and reliability. Vacuum chamber testing, or thermal vacuum testing, is one of the key space qualification parameters. The method replicates the temperature and pressure conditions to validate the design of components and uncover hidden flaws within the material or assembly.

The space components experience ultra-high vacuum, extreme temperature variations, and the absence of convective heat transfer. Therefore, the tests must be conducted in such a way that they resemble these conditions to ensure mission readiness and long-term survivability.

Vacuum chamber testing serves several key purposes:

- Thermal balance verification: Confirmation of thermal model predictions at steady-state or transient space-like conditions.
- Thermal cyclic endurance: Simulating expansion/contraction fatigue by numerous thermal cycles.
- Outgassing assessment: Avoiding outgassing of volatiles in vacuum that could contaminate sensitive surfaces (e.g., optics or sensors).
- Design weaknesses detection: Analyzing for flaws in mechanical interfaces or wiring that only exists under stress due to temperature extremes and pressure gradients.

**Standards and Regulations**

Several well-established international standards define procedures, conditions, and acceptance criteria for vacuum chamber testing of space components.

ECSS – European Cooperation for Space Standardization

The ECSS-Q-ST-70-04C, ECSS-Q-ST-70-02C standards and ECSS-E-HB-31-03A handbook provide detailed instructions for environmental testing, including vacuum chamber testing procedures for aerospace hardware. Key points of interest include [8], [9], [10] :

- Specified thermal cycle periods and limits (e.g., soak time at extreme temperatures)
- Vacuum range classification (high, ultra-high)
- Outgassing acceptance criteria based on TML (Total Mass Loss) and CVCM (Collected Volatile Condensable Materials) limits. TML must not exceed 1.00 % and CVCM must be below 0.10 %
- Test durations sufficient to cover thermal transients and verify stability
- Temperature monitoring, sensor redundancy, and calibrated data acquisition systems requirements

NASA GEVS (General Environmental Verification Standard)

NASA GEVS GSFC-STD-7000A is a widely used standard for environmental testing of spaceflight hardware. It gives general guidelines for vacuum chamber testing such as [11]:

- Minimum 2-4 thermal cycles, unless otherwise justified
- Vacuum pressure typically below $1 \cdot 10^{-5}$ Torr
- Soak time sufficiently long to reach thermal equilibrium (steady state)
- Controlled temperatures ramp to avoid mechanical stress
- Contamination monitoring with witness plates or quartz crystal microbalances

Vacuum chamber tests are key in the environmental qualification process of aerospace components. By simulating the thermal and vacuum conditions of space, engineers then test system performance, find hidden weaknesses, and thus gain confidence in mission success. Regulatory frameworks (e.g., ECSS and NASA GEVS) offer various structured methodologies to maintain reliability, repeatability, and traceability of the test.

# 2 State-of-the-art

## 2.1 Thermal Vacuum Chamber

### 2.1.1 Main Setup

The development of the Thermal Vacuum Chamber (TVAC) started at the Institute of Aerospace Engineering, BUT in 2014 [12]. Until now, four versions of the chamber were developed: Version 1, Version 2 initial, Version 2 advanced and Version 3. Version 3 chamber is currently used for tests of the specimens. The most important parameters of TVAC Version 3 are described in Table 2.1. In order to accommodate future upgrades and meet all the initial criteria, the Thermal Vacuum Chamber was designed as a modular facility. The maximum operational temperatures for components of the TVAC that are influenced by high temperatures on hot interface during testing (HF sensor, resistors, thermocouples and glue for thermocouple installation) can be seen in Table 2.2.

*Table 2.1 Parameters of the TVAC [13]*

| Parameters | Values |
|---|---|
| Inner environment pressure range | $1x10^{-5} \div 1x10^{5}$ Pa |
| CI temperature range | -150 ÷ 100 °C |
| HI temperature range | -125 ÷ 100 °C |
| Inner volume | 5.5 $dm^3$ |
| Weight | 55 kg |
| Dimensions (LxWxH) | 530 x 344 x 393 mm |
| Dimensions with systems (LxWxH) | 713 x 344 x 509 mm |

*Table 2.2 Maximum operating temperatures of selected components [13], [14], [15]*

| Components | | Temperature | |
|---|---|---|---|
| HF Sensor | | 150 | °C |
| Resistors | | 150 | °C |
| Thermocouples | | 300 | °C |
| Glue X60 | stat.<br>dyn. | 60<br>80 | °C |

The main component of the TVAC is a T-shaped part made of stainless steel. On the left side of this T-shaped part is a screwed-on large flange with HI LIN tank connection, vacuum pump connection, vacuum feedthrough and pressure gauge connection. On the right side is also a screwed-on large flange with CI LIN tank connection and two vacuum feedthroughs. The HI and CI liquid nitrogen tanks are used for storing liquid nitrogen, that was chosen as a coolant. On top is a smaller flange used for $CO_2$ feed and for easier manipulation in the TVAC. At the front is also a smaller flange for easier manipulation inside the TVAC and includes a window for monitoring during testing. For stability of the TVAC, two legs are connected to the side flanges.

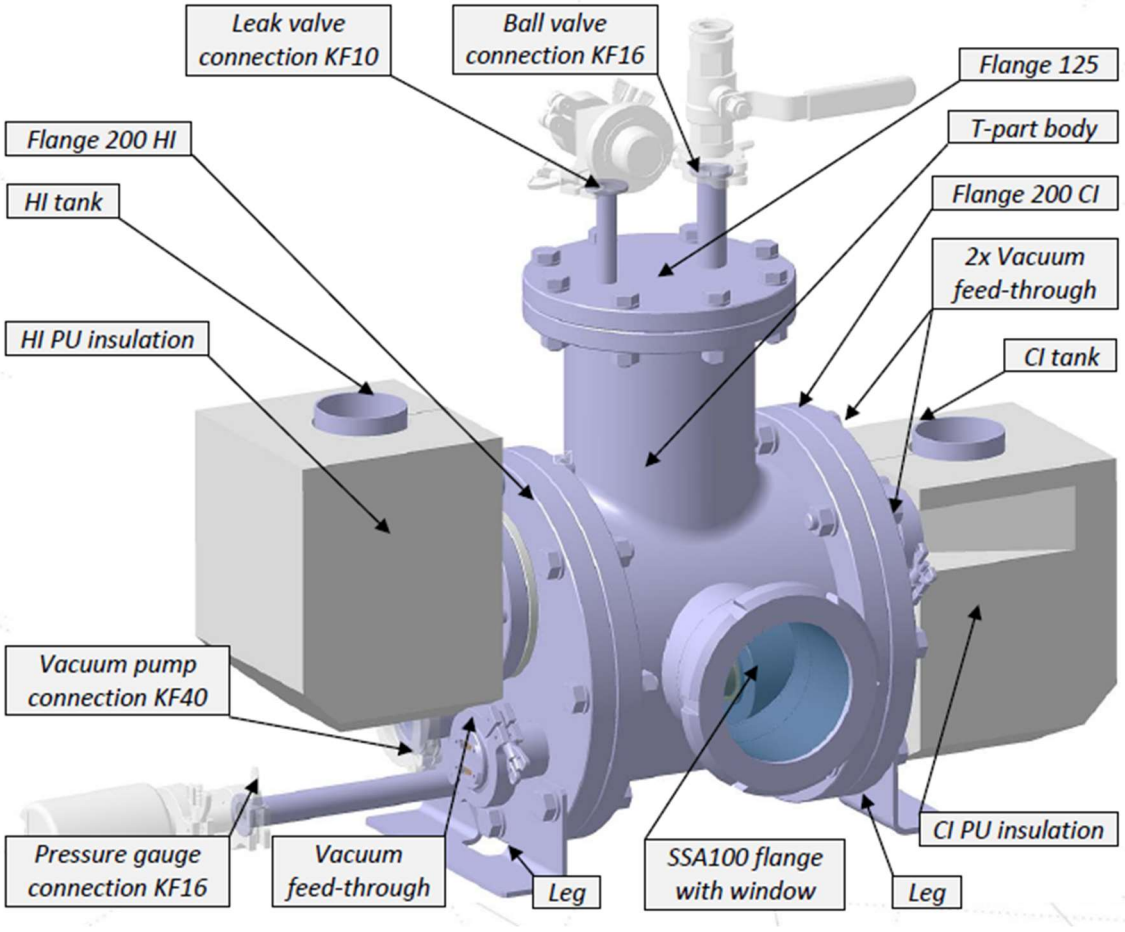


*Figure 2.1 TVAC - outer parts [13]*

The inner composition of the TVAC can be seen in Figure 2.2. The tested specimen is positioned between a hot copper plate (HCP) and cold copper plate (CCP). The HCP and CCP serve as substitutions for heat-dissipating equipment and a heat sink. Under the CCP is a Cold interface, which is connected to the CI LIN tank through the CI rod. The Hot interface, if needed, can also be cooled down using HI LIN tank. For that, four copper belts leading from HI rod and connected to the Hot interface are used. On top of the HI, a PTFE weight pad is placed together with the Weight. This weight increases the pressure and improves the contact conditions between Hot interface and Cold interface.

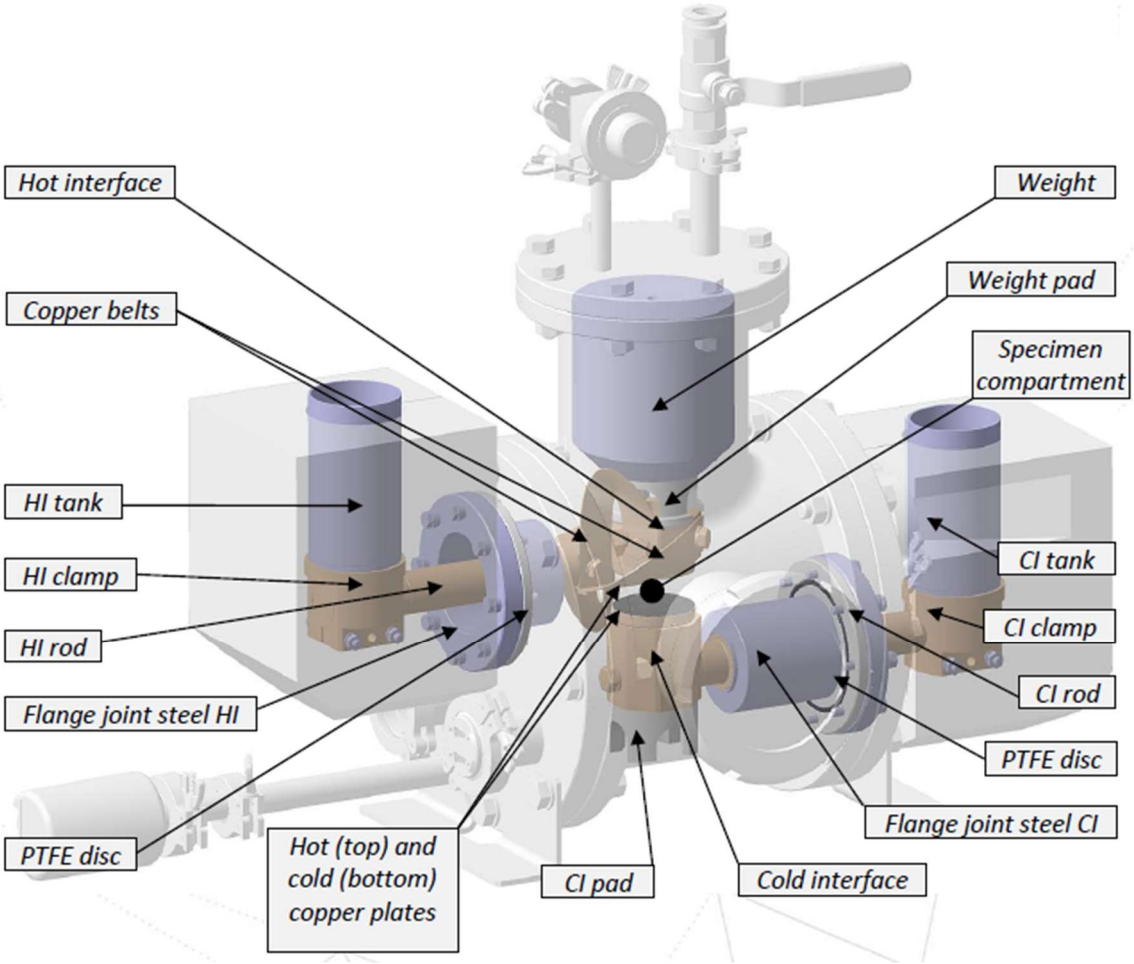


*Figure 2.2 TVAC - inner parts [13]*

The insulation of the TVAC can be seen in Figure 2.3, where green color indicates a PTFE insulation (with minimum 10 layers) and purple color indicates thermal multi-layer insulation (MLI).

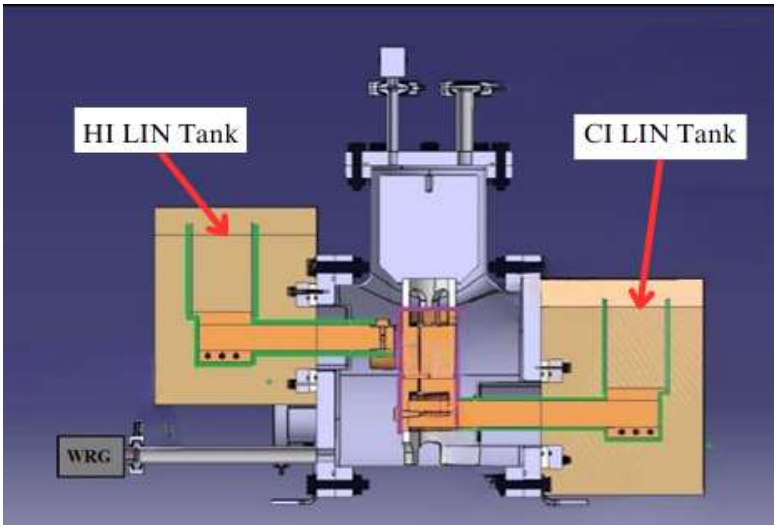


*Figure 2.3 TVAC cross section (isolation) [12]*

**Configurations**

The inner parts of the TVAC (HI, HCP, CCP and CI) can be changed to a different configuration based on specific needs and requirements for the testing. The installation of a heat flux sensor, connection of the copper belts to HI and change of the position of the thermocouples are part of the subsystem configuration alterations. The three main configurations with the main changes are depicted in Figure 2.4. The configuration 1b compared to the other two includes the heat flux sensor between HI and HCP. The configuration 2 has four copper belts connected to HI.

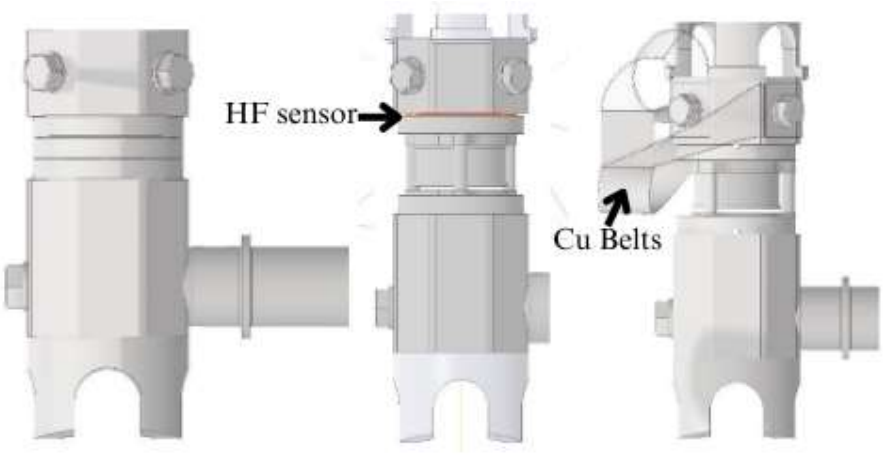


*Figure 2.4 Configurations of the TVAC (from the left: 1a, 1b & 2) [13]*

## 2.1.2 TVAC Systems

In this chapter, the systems, subsystems and equipment of the TVAC are described. Photo documentation for each individual part can be found in Appendix A1.

**Mechanical System**

The mechanical system consists of the main body described in Chapter 2.1.1 and electrical vacuum feedthroughs, that provide connection between sensors in vacuum chamber and data acquisition unit ESAM Traveller.

**Pressure Control System**

The evacuation of the air out of the TVAC is provided by turbo-pumping station. This turbo-pumping station is controlled by Turbo Instrument Controller (TIC). The station is connected to TVAC with tube with a Ball valve 1. The Ball valve 2 connected to top flange of the TVAC is designed for emergency pressurization of the chamber. For pressure measurement, active wide range gauge (WRG) is used, with ability to measure pressure from atmospheric pressure to $10^{-7}$ Pa.

For the tests conducted with $CO_2$, $CO_2$ tank with reduction valve is used. The leak valve connected through tube with reduction valve provides fine control of the $CO_2$ feed to the chamber.

**Temperature Control System**

For heating, four resistors with resistance of 8 Ω, connected series-parallelly (scheme is in Figure 2.5), are installed in hot interface and cold interface. The DC relay is used for controlling the current in resistor circuit. Two relays are used, one for HI resistor circuit, one for CI resistor circuit. The input is from the PID regulators and output is connected to the resistor circuit.

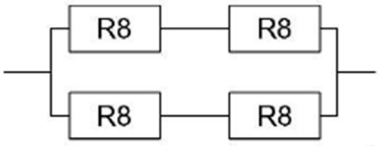


*Figure 2.5 Series-parallel scheme of resistors [13]*

Two programmable PID regulators are used in the TVAC system. The inputs for the regulators are TH5 thermocouple for HI regulator and TC5 thermocouple for CI regulator. The HI regulator controls the temperature on HCP and CI regulator the temperature on CCP.

For powering the HI DC relay, DC power supply that allows regulation of the input current and voltage is used. For CI DC relay unregulated power source is used.

As temperature sensors Pt100 thermocouples are used in a three-wire line configuration to increase the precision of the temperature measurement. The location of all thermocouples is described in Table 2.3 and placement of the thermocouples inside the TVAC can be seen in Figure 2.6.

*Table 2.3 Location of thermocouples [13]*

| Location | Thermocouples |
|---|---|
| HI | TH8 |
| HCP | TH2, TH3, TH4, TH6, TH7 |
| CCP | TC2, TC3, TC4, TC6, TC7 |
| CI | TC8 |
| Outer wall | TO1, TO2, TO3 |
| Inner wall | TC1 |

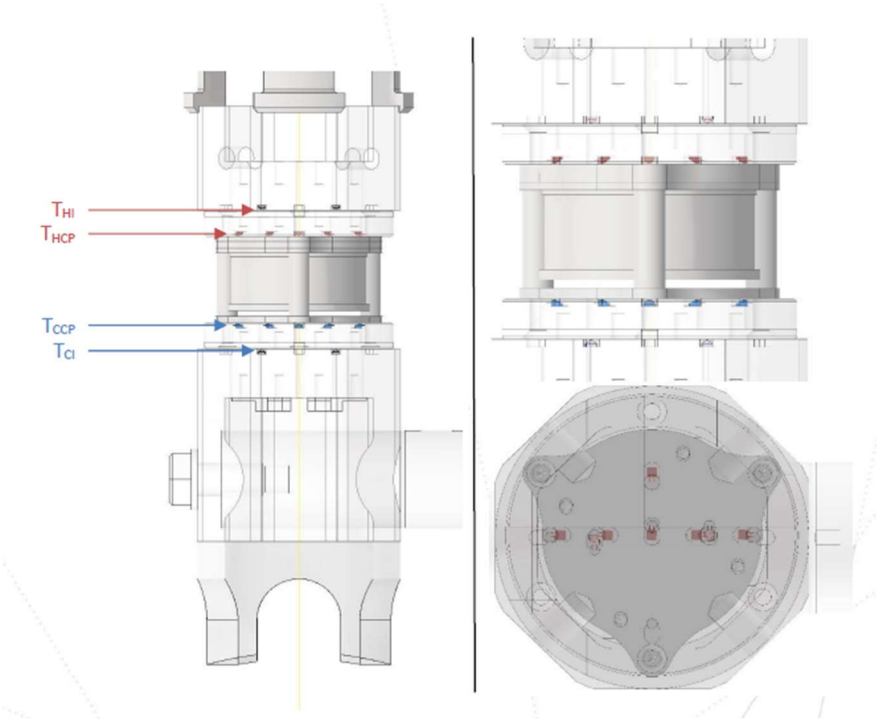


*Figure 2.6 Position of inner thermocouples [13]*

For measuring heat flux, FHF02 Hukseflux is used. It is applicable over a temperature range from -40 to +150 °C. FHF02 measures heat flux from conduction, radiation and convection. The sensor in FHF02 is a thermopile, that measures the temperature difference across the body of FHF02. A type T thermocouple is integrated as well. [14]

Liquid nitrogen is used as a coolant for tests. It is stored in an isolated tank with overpressure control, but even when it is not in use, its supply is depleted in a few days.

**Data acquisition System**

Meaningful conclusions can only be drawn from experimental results when data evaluation is performed accurately and reliably. Therefore, this chapter describes comprehensively all data handling procedures for this study that are associated with acquisition, storage, and preprocessing. The intention of this chapter is to ensure that all experimental data are treated systematically and that the results taken for analysis in the later chapters are fully traceable.

Large datasets were produced throughout all the tests including temperature profiles on HI & CI, heat flux measurements and pressure values. The various conditions of testing such as $CO_2$ and vacuum environment required strict and uniform data evaluation procedures. The evaluation structure was supported by a thermal model that assured accuracy and comparability in measurement results.

## Data Acquisition and Storage

The ESAM Traveller is a data acquisition system (DAS) unit that allows continuous data transfer with up to 8 MB/s via USB 2.0 port [16]. Channel identification is quickly selectable and changeable. The DAS unit requires separate power source. Data measured with a sampling rate of 0.1 Hz (every 10 s) from temperature sensors, heat flux sensor and wide range gauge are sent to the DAS and displayed on a computer with ESAM software.

Data were saved as space-separated values in .txt format, which allows easy import into analysis software (in our case, thermal model in Excel), using Text Import Wizard. Each dataset was assigned a unique Test ID with data detailing environmental conditions (gas type, heat load), type of test and timestamp. Backup copies of all raw data were stored on cloud storage to assure integrity and prevent loss.

## Thermal Model

To support data interpretation, a thermal model created in Microsoft Excel was used. This model was originally developed in an older master's thesis at IAE [12, pp. 41–49] and for this thesis was slightly adjusted. This model simulates the thermal behavior of the test setup based on parameters such as material properties and boundary conditions. It is a theoretical reference point for analysis of measured data and verification of thermal resistance and conductance values obtained from measurement.

This chapter describes only basic information about the thermal model and the details are described in thesis [12] mentioned in the previous paragraph.

The measured raw data from the tests that are imported to the model and used for calculations are:

- Temperature: TH2-TH8 & TC1-TC8, outside temperatures (TO1-TO3), temperature on HF sensor
- Voltage: voltage from WRG and HF sensor

The parameters are always calculated in a steady state using the following equations:

- Average temperature on HCP ($T_{Hot}$)

$$T_{Hot} = \frac{T_{H2} + T_{H3} + T_{H4} + T_{H6} + T_{H7}}{5} \tag{2.1}$$

- Average temperature on CCP ($T_{Cold}$)

$$T_{Cold} = \frac{T_{C2} + T_{C3} + T_{C4} + T_{C6} + T_{C7}}{5} \tag{2.2}$$

- Temperature difference between HCP and CCP (dT)

$$dT = T_{Hot} - T_{Cold} \tag{2.3}$$

- Heat Flux (HF)

$$HF = \frac{U}{\left(k \cdot \left(1 + 0.025 \cdot (T_{sp} - 20)\right)\right)} \tag{2.4}$$

  - U is voltage measured by heat flux sensor
  - k is heat flux sensor sensitivity constant equal to $5.5 \cdot 10^{-6}$ [V/(W/m$^2$)] [14]
  - $T_{sp}$ is the temperature measured on the specimen
- Input power ($Q_{in}$)

$$Q_{in} = HF \cdot A_{HCP} \tag{2.5}$$

  - $A_{HCP}$ is the area over which the heat flux is considered (=2258.99$\cdot 10^{-6}$ mm$^2$)
- Total resistance ($R_{tot}$)

$$R_{tot} = TCR + R_{sp} = TCR_1 + R_{sp} + TCR_2 \tag{2.6}$$

  - $R_{sp}$ is resistance of specimen
  - TCR is thermal contact resistance and is a sum of $TCR_1$ and $TCR_2$
- Specimen conductance ($C_{sp}$)

$$C_{sp} = \frac{Q_{in}}{dT - (TCR \cdot Q_{in})} = \frac{1}{R_{tot} \cdot TCR} \tag{2.7}$$

- Thermal contact conductance (TCC)

$$TCC = \frac{2}{\left(R_{tot} - \left(\frac{1}{C_{sp}}\right)\right) \cdot A_{sp}} \tag{2.8}$$

  - $A_{sp}$ is the area of specimen

The thermal model also provided a visual representation of evaluated test and quality evaluation of steady state.

Although this model is relatively simple, it proved important during plausibility checks of measured heat flux and temperature profiles and for the final evaluation of the specimen's thermal parameters.

## 2.2 Dummy Design

For this thesis test campaign, two dummy specimens were used to simulate interface conditions in a space-representative, controlled test environment. The dummies served as substitutes for miniaturized heat switch (MHS), allowing the testing of heat transfer behavior in conducted tests. By using dummies, safe and repeatable measurements could be made without complexity or risks associated with operational components. Both dummies were developed in previous projects at IAE and the development of them is not a part of this thesis goals. This chapter serves as a basic introduction of both dummies and the application of them in tests.

**Purpose and Role of the Dummy Specimens**

The dummy specimens were used as the central thermal interface element in the test stack. Their main task was to provide a stable and well-defined thermal path between the hot and cold interfaces. The dummies were not intended to simulate all aspects of the miniaturized heat switch.

**Properties of Dummies**

Two dummies were used, each made from a different material. The first dummy is made from bronze ($CuSn_8$), and the second dummy is made from aluminium alloy (Al 7075 T73).

The geometry of the bronze dummy can be seen in Figure 2.7, where on the left side are exact dimensions and on the right side is an isometric view of the specimen. The top and bottom parts have a diameter D=45.7 mm and area A=1626.8 $mm^2$ each.

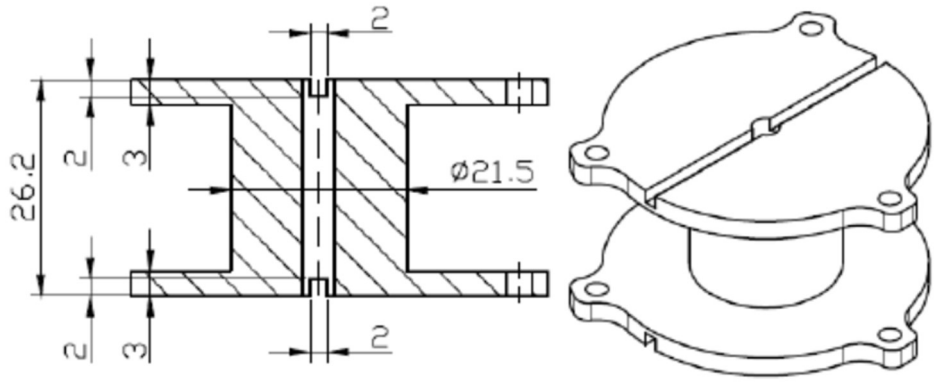


*Figure 2.7 Bronze ($CuSn_8$) dummy [12]*

The geometry of the aluminium dummy can be seen in Figure 2.8. Similarly to previous figure, on the left side are exact dimensions and on the right side is an isometric view of the specimen. The area of the aluminium specimen is equal to A=1911.3 $mm^2$.

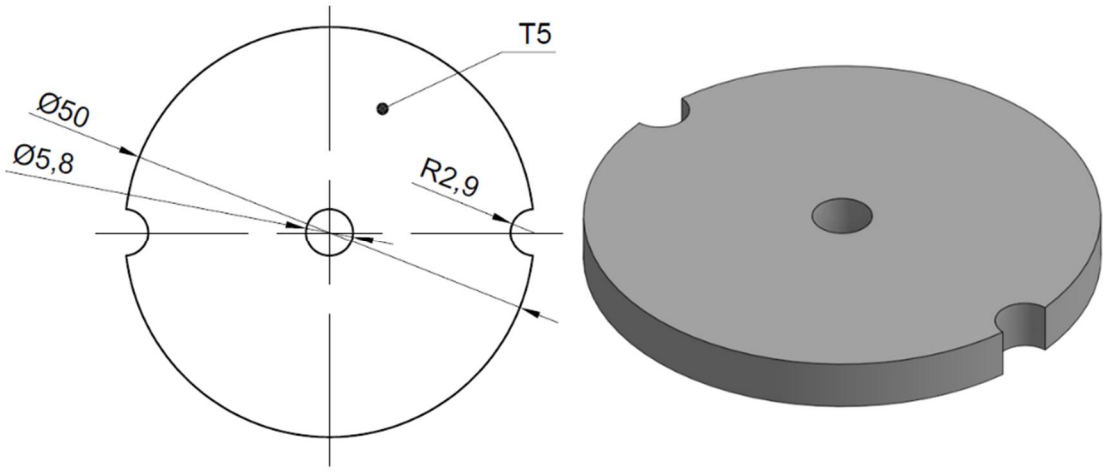


*Figure 2.8 Aluminium (Al 7075 T73) specimen*

**Application in Tests**

The bronze dummy is used in pilot tests, both in vacuum and $CO_2$ atmosphere and for the vacuum and $CO_2$ cyclic tests (tests IDs 1000 to 1005). The aluminium dummy was used in tests with ID 1006 to 1011, conducted in vacuum.

**Mounting and Integration**

Each dummy was placed in TVAC between hot copper plate and cold copper plate. When using the bronze dummy, contact was established by screwing it together with HCP and CCP to maintain stable position during testing.

## 2.3 Test-type Specification

### 2.3.1 Cyclic Tests

**Objectives**

The main objective of the cyclic tests is to evaluate the performance of the test specimen (in this case $CuSn_8$ dummy) when subjected to multiple thermal cycles. The vacuum cyclic test simulates space-relevant environment (pressure and temperature conditions). The goal of the $CO_2$ cyclic test is to recreate conditions for a Mars mission (in 1000 Pa $CO_2$ atmosphere and fluctuating temperature).

Before the actual tests, two preliminary feasibility vacuum tests were conducted to find out if cyclic testing was possible. The aim of these preliminary tests was to analyze the ability of cooling down and heating in TVAC in required time and maintaining the temperature difference at hot and cold peak temperatures. This involves finding out the necessary power output of HI power source and estimation of amount of liquid nitrogen used.

**Identification of Test Requirements**

The requirements for the cyclic tests were established on both previous theoretical descriptions (described in [17, p. 45]) and observations from the feasibility tests. The successful realization of the tests relied on the completion of different environmental and procedural conditions:

Environmental Conditions:

- One test conducted in vacuum ($<10^{-3}$ Pa).
- One test conducted in $CO_2$ atmosphere at 1000 Pa.
- Repeating thermal cycling for both tests between -135 °C and 60 °C on CI and -65 °C and 70 °C on HI.

Procedure Requirements:

- Dwell times of 1 h and ramp rates of 2 hours for cooling and 2 hours for heating (equal to temperature gradient of 1.625 °C/min for CI and 1.125 °C/min for HI) were chosen based on thermal response observed during the feasibility tests.

**Test Profiles**

The anticipated temperature profiles of the hot and cold interfaces based on the test requirements are in Figure 2.9. These profiles illustrate the time-dependent temperature behavior of the environment both during vacuum cyclic testing and in $CO_2$ atmosphere conditions.

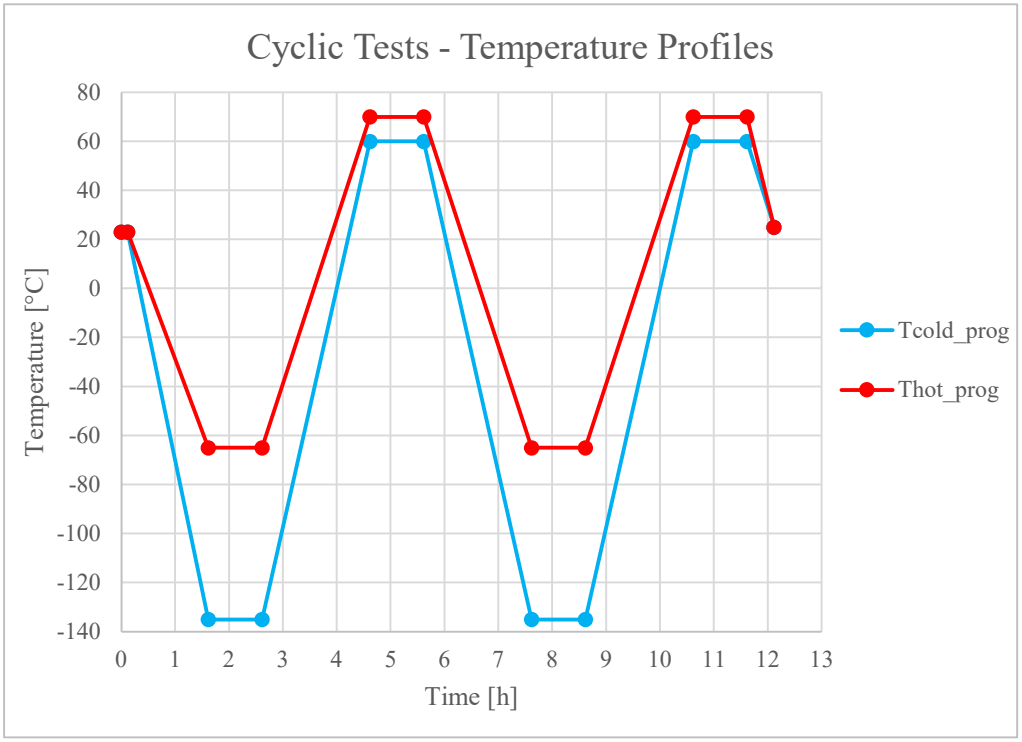


*Figure 2.9 Anticipated test profile of cyclic tests*

### 2.3.2 Thermal Balance Tests

**Objectives**

The main goal of the tests conducted with the aluminium dummy is to determine the thermal contact resistance (TCR) between the specimen and the hot/cold copper plate (HCP/CCP). To evaluate the TCR (and other thermal values), steady state in thermal vacuum chamber needs to be reached. Execution of these tests, where the interfaces are made from two different metals (aluminium and copper), can be useful for aerospace applications.

These tests were designed to create a steady-state conditions, in which total thermal resistance and total thermal conductance (TCC) can be determined. Unlike the cyclic tests, this phase of test campaign focused on steady-state performance alone, allowing the thermal contact behavior of the aluminium specimen to be investigated more closely, without the effects of cyclic thermal loading.

**Identification of Test Requirements**

Based on previously carried out tests and to ensure reliable measurement of TCC, the test setup had to achieve several requirements:

Environmental Conditions:

- The tests were realized in high vacuum ($<10^{-3}$ Pa).

Thermal Boundary Conditions:

- A defined temperature on cold interface was maintained (limit of ±0.5 °C) with stable dwell times to guarantee thermal equilibrium.

**Test Profiles**

The aluminium tests consisted of two steady-state temperature profiles. The cold interface was actively cooled to target temperature (for regulated tests) and after powering the HI power source, the temperature on hot interface gradually increased/decreased to reach steady state. The required time in steady state for all tests was a minimum of one hour. Figure 2.10 is an example of test profile of regulated thermal balance test, the actual tests are conducted at different temperatures. In Figure 2.11 is test profile of unregulated thermal balance test.

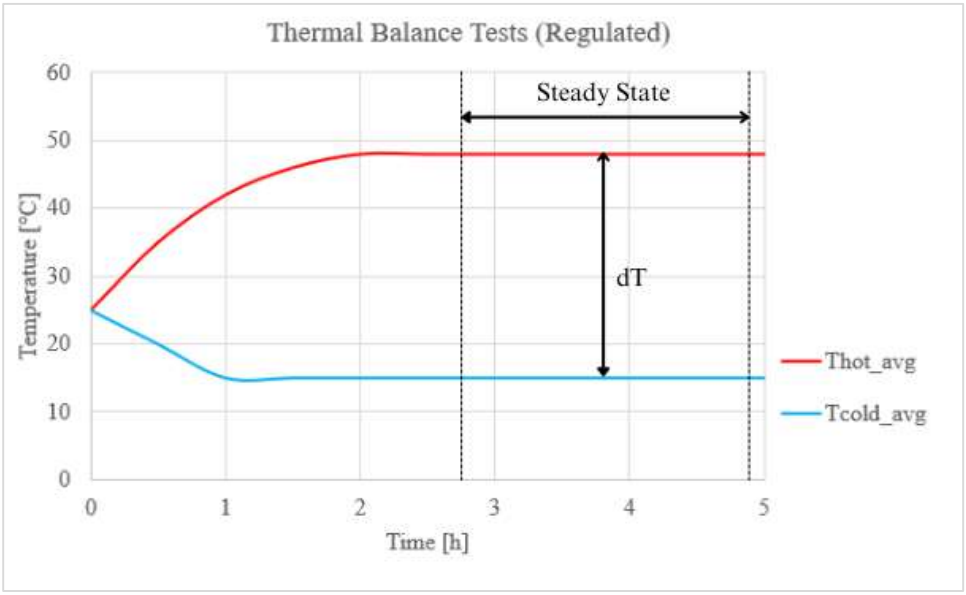


*Figure 2.10 Exemplary test profile (regulated thermal balance tests)*

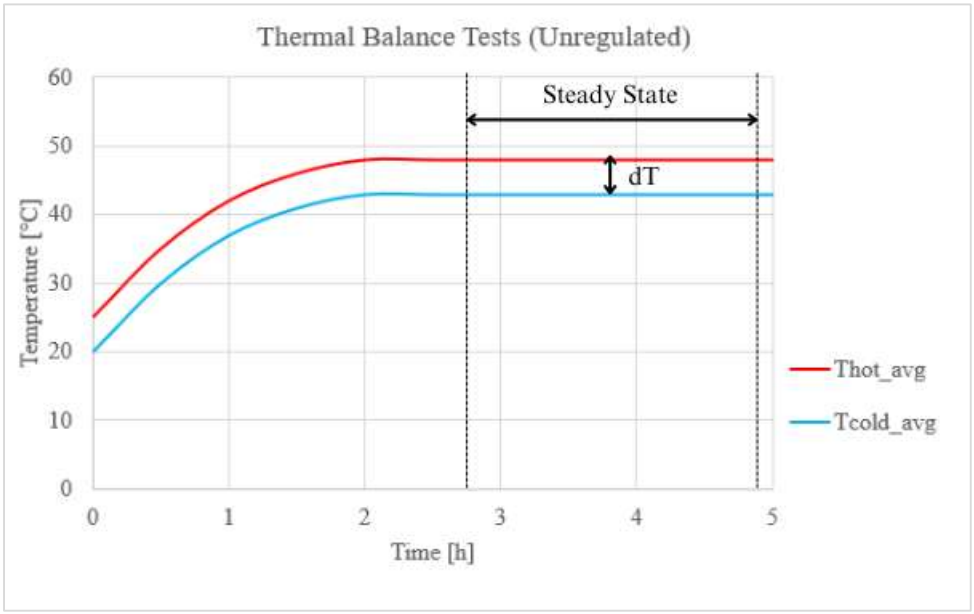


*Figure 2.11 Exemplary test profile (unregulated thermal balance tests)*

## 2.4 Steady-State Criteria

The steady state of thermal vacuum chamber (TVAC) is considered a chosen time frame during testing, in which the temperature variation on hot copper plate (HCP)-$T_{Hot}$ and cold copper plate (CCP)-$T_{Cold}$ is less than 0.5 °C/s [13]. After 60 minutes with constant development of temperatures on HCP/CCP, the start of the steady-state period is considered. The length of the steady-state period should be at least 60 minutes [13]. Throughout the selected period of steady state, a steady heat flux across the measurement assembly is assumed. The steady state of the TVAC can be controlled or uncontrolled. The controlled steady state must be manually maintained by adding liquid nitrogen to the liquid nitrogen tanks of the TVAC. The

uncontrolled steady state is reached naturally, without regulating the temperature with liquid nitrogen. It also takes longer time to reach an unregulated steady state.

The steady state requirements are [13]:

- The maximum fluctuation of $T_{Hot}$ and $T_{Cold}$ temperatures is ±0.5 °C.
- The minimum time period of constant $T_{Hot}$ and $T_{Cold}$ temperatures is 60 minutes.

# 3 Background and Objectives of Work

Prior to this thesis, several test campaigns were carried out with the aim to have fully calibrated TVAC for miniaturized heat switch (MHS):

- Thermal vacuum chamber validation experiments. [17]
- Calibration measurements of bronze specimen, including regulated thermal balance tests with different power inputs and temperatures on cold interface. [12]
- Thermal balance tests with copper specimen, both regulated and unregulated and in vacuum and $CO_2$ atmosphere were conducted. [18]

The primary goal of the thesis was to prepare the test setup and data evaluation process for calibration and qualification in the future for the miniaturized heat switch. This was to guarantee that the system could accurately measure thermal variables in controlled conditions and to withstand thermal loads during repeatable heating and cooling.

For this purpose, the following goals were set:

- Perform a series of pilot tests to validate temperature control, sensor stability, and test procedure feasibility in vacuum and low-pressure $CO_2$ conditions.
- Develop and execute cyclic tests to assess the stability and reproducibility of tests under thermal loading representing operating conditions.
- Perform thermal balance tests with aluminium specimen to analyze the effect of materials on thermal contact resistance and help define baseline behavior.
- Refine and apply the thermal model to interpret experimental data from tests with different conditions

In doing so, this work is a direct continuation of the earlier developments. The outcome of this thesis represents the next step in experimental verification and methodological clarity to facilitate future testing and calibration for miniaturized heat switch.

# 4 Test Methodology

This chapter outlines the overall methodology taken for the pilot tests, cyclic thermal tests and thermal balance tests. It provides the structure and technical basis for the conducted experiments. This chapter includes the test setup modifications, risk assessment and mitigation strategies, the success criteria adopted to evaluate the results, data validation checks, preparation for further analysis, pre-test checklist, and post-test checklist. Together, they create the grounds for the execution and interpretation of all the tests conducted for this thesis.

## 4.1 Test Setup Modifications

**Cyclic Tests**

This subchapter defines the significant aspects of test setup used for cyclic thermal testing and the changes made when switching from the TVAC configuration 1b to TVAC configuration 2.

The most important change was the 4 copper belts (on the left side in Figure 4.1 are securely fastened, to not take up space during other tests). These belts have been screwed on HI using 4 copper screws. This modification was made to improve the temperature control and environmental consistency during cyclic testing.

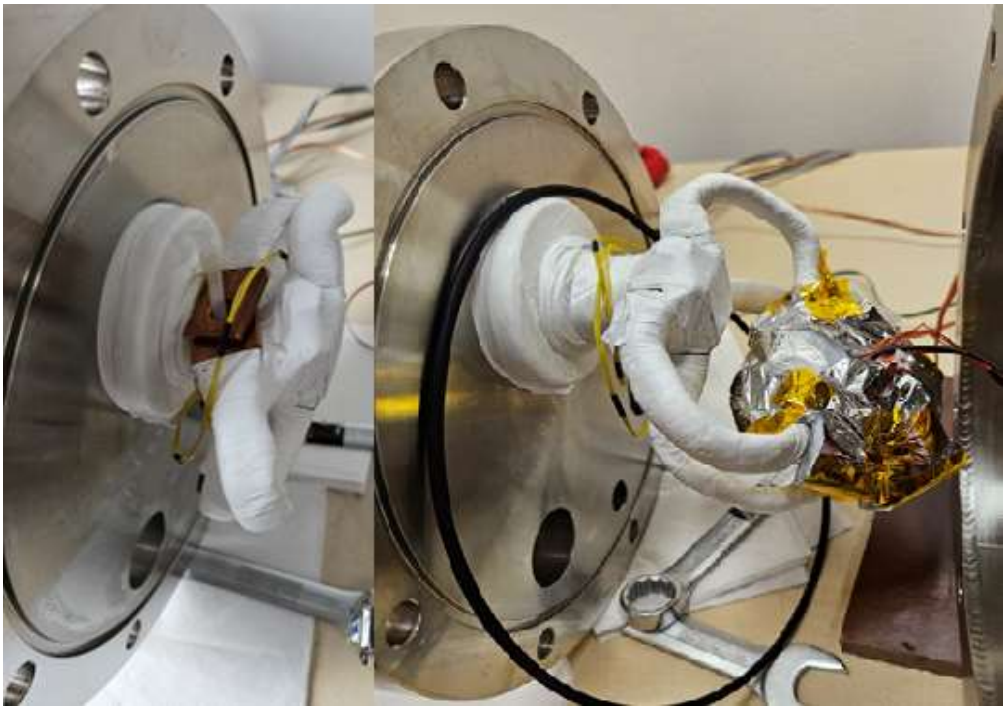

*Figure 4.1 Copper belts – disconnected (left side) and connected (right side)*

To lower the consumption of liquid nitrogen, Styrofoam covers for both the HI and CI LIN tanks were added, secured with Kapton tape (Figure 4.2).

*Figure 4.2 Isolation of LIN tanks*

For maintaining a defined thermal gradient and preventing lateral heat loss, new insulation was developed (Figure 4.3). The HI was insulated with MLI to cover the sides and the top and fixed with Kapton tape. Also, 4 squares of MLI were added on top of the copper screws, to properly insulate the HI. This top part insulating the HI had larger diameter than the bottom part of the insulation. That is because the top part was during assembling put on the bottom part, something like a "cap". The bottom part insulation was the same as during the pilot testing.

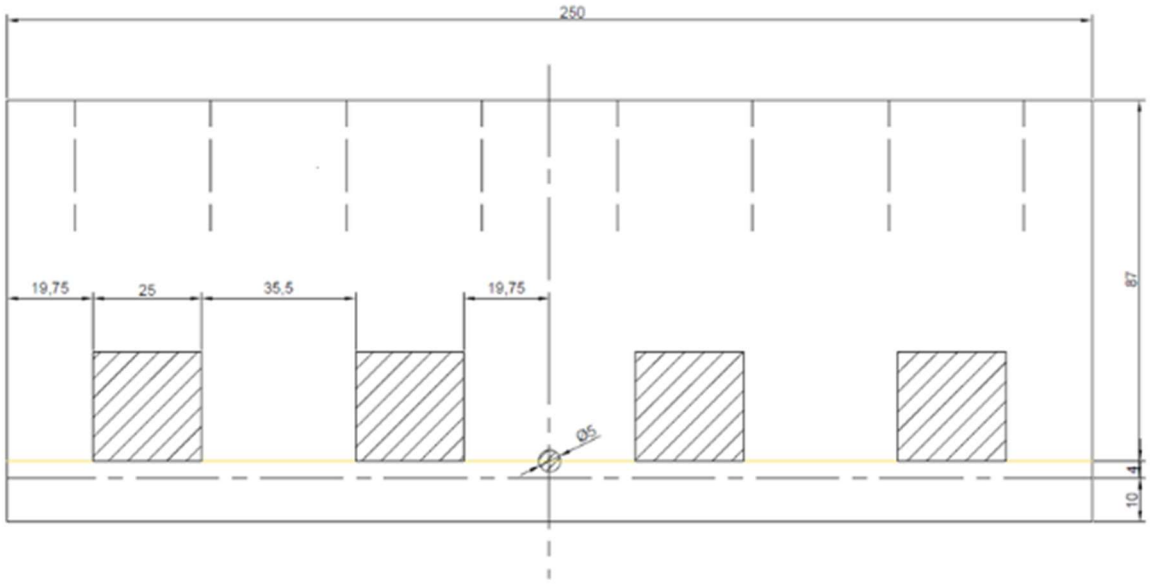


*Figure 4.3 Insulation of hot interface (HI)*

**Thermal Balance Tests**

The thermal vacuum chamber for tests with aluminium specimen is in configuration 1b, equivalent to configuration in pilot tests. The test stack with specimen on top and the whole test stack can be seen in Figure 4.4. This picture shows that the specimen is not fixed in any way to the rest of the stack.

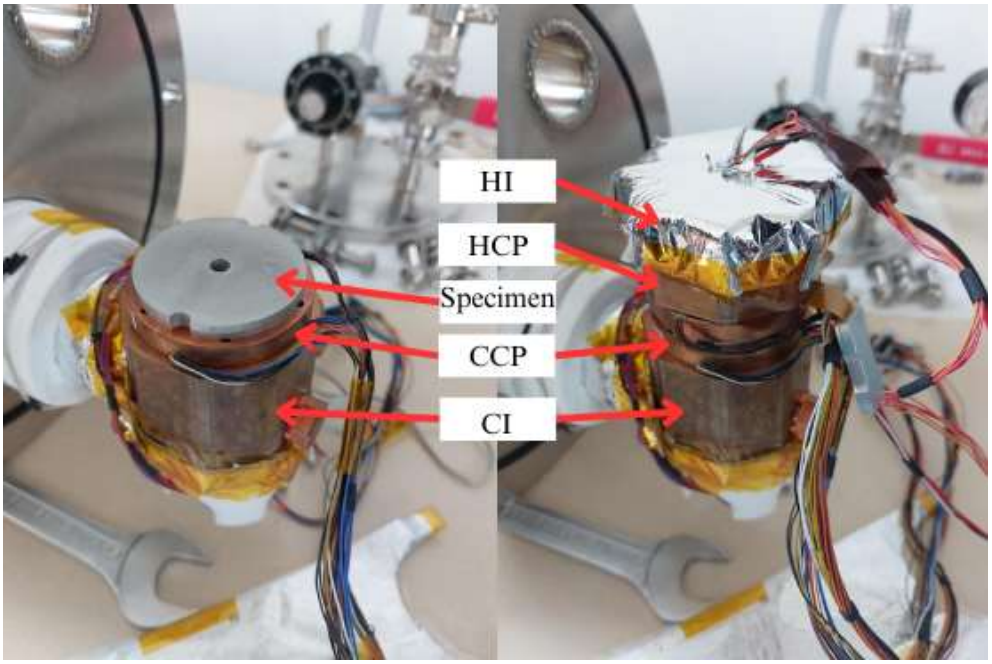


*Figure 4.4 Test stack for thermal balance tests*

The insulation of the test stack is as follows: As in test setup of cyclic tests, on HI is the "cap", that covers it from top and from the sides, with cutout for cables leading from HI, but without the squared cutouts for belts connection. Then, the whole test stack is covered with MLI, with cutouts for cables from HI, HCP, heat flux sensor, CCP and CI.

After the cyclic tests, it was found that cables leading from temperature sensor TH8 and cables leading to one branch of resistors on HI were damaged. This incident happened during manipulation of the test stack after the cyclic tests. The damaged cables were desoldered and replaced with new ones, that were soldered back.

## 4.2 Risk Assessment and Mitigation

**Cyclic Tests**

The risks associated with cyclic thermal testing include both operating and hardware-related issues. In the next paragraph are identified risk areas along with mitigation strategies, that can be enforced in the future cyclic testing.

The first risk involves mechanical damage to sensor cables during installation of the specimen. This poses a threat to data integrity, in the sense that damaged or disconnected cables could lead to incomplete measurements or loss of signal. To mitigate this risk, additional care should be taken to handle the specimen, with cable routing secured. After installation is finalized, there should be minimal manipulation with the specimen.

The second risk is overly high temperatures on the hot interface, leading to sensor damage (heat flux sensor) as well as damage to the resistors. This can be avoided by monitoring the temperatures in real time in ESAM software and by avoiding higher power outputs from the HI

power source, that would prevent the temperatures from exceeding the predetermined maximum temperatures.

**Thermal Balance Tests**

While the test procedure for the thermal balance tests was simpler than that of the cyclic tests, certain risks were identified that might affect the replicability and precision of thermal contact resistance measurements.

The first and second risks identified are the same as in cyclic testing described in second and third paragraph – mechanical damage to sensor cables during manipulation of the test stack (or part of it) and overly high temperatures on the hot interface.

The third risk is related to the aluminium dummy not being screwed to HCP or CCP but was mechanically compressed inside the test stack. While this allowed simpler and quicker test setup, it introduced the possibility of uneven contact pressure. This would affect the reproducibility of the thermal contact quality and bring uncertainty into the measured temperature gradient within the stack. To mitigate this risk the specimen was precisely centered between the copper plates, and the test stack was optically inspected before the TVAC was sealed.

## 4.3 Success Criteria

**Cyclic Tests**

The cyclic tests success was defined by a series of performance and consistency criteria, all of which were supported and validated by preliminary feasibility tests and vacuum and $CO_2$ cyclic tests. The following success criteria were identified:

- Environmental stability: Strict control and maintenance of temperature (both on HI and CI) and pressure conditions in vacuum and $CO_2$ tests.
- Data integrity: Complete sets of data with no sensor failures, signal drift, or major discontinuities.
- Procedural reliability: Successful application of a repeatable, validated procedure that can be applied during future test campaigns.

These criteria guarantee the test results are both scientifically reliable and of practical value for space-representative thermal testing.

**Thermal Balance Tests**

The thermal balance tests were considered successful if the following criteria were met:

- Thermal stability: Temperature and heat flux measurements remained stable for a sufficient period to allow reliable steady-state analysis.
- Sensor reliability: There was no signal loss, drift, or no abnormal readings appeared during the data acquisition period.

- Consistency with expectations: Calculated TCR values were in the physically feasible range based on material properties and contact mechanics.

## 4.4 Data Validation and Consistency Checks

To ensure calculated parameters consistency, several validation procedures were employed:

- Reproducibility Checks: Repeating the tests under identical conditions provided less than 5% variation, indicating good repeatability.
- Cross-Validation: Measurements conducted in vacuum and $CO_2$ atmospheres were compared to detect any systematic deviations.

## 4.5 Preparation for Further Analysis and Interpretation

After validation, the processed data were organized into tables categorized by Test ID, test environment and experimental conditions. These datasets represent the foundation for the subsequent chapters, particularly those that involve experimental validation and discussion. The precision and reliability established within this stage ensures that the conclusions deducted later in the thesis are based on thoroughly assessed and reproducible evidence.

## 4.6 Pre-test Checklist

**System Connection and Startup Procedure**

1.) Power Connection
   Ensure the following devices are properly connected to the main power source:
   a) HI power source
   b) CI power source
   c) Vacuum pump station
   d) HI temperature regulator
   e) CI temperature regulator
   f) ESAM power source
   g) PC
2.) ESAM - Inputs and Channels Setup
   a) Connect all temperature channels
   b) Connect TIC pressure channel
   c) HF sensor temperature and voltage channels (in 1b configuration)
   d) ESAM's power source
3.) Data Connection
   Connect the ESAM USB output to the PC.
4.) HI/CI Regulators Input Connection
   a) Input temperature (TH5 & TC5)
   b) Heating resistors input
5.) Power Output Configuration
   a) The output from the regulators must be connected to the HI/CI power source

6.) TVAC Tightness Check
   a) Verify the screw tightness of the CI flange 200, HI flange 200 and top flange 125
   b) Check the proper helix tightening of the SSA 100 window
   c) Open Ball Valve 1 (vacuum pump connection)
   d) Ensure the Leak Valve is closed
   e) Verify that Ball Valve 2 (top flange) is closed

**System Power-Up**

1.) ESAM Activation
   a) Power on the ESAM's power source
   b) Power on the ESAM unit
2.) Vacuum Pumping Station Setup
   a) Switch on the TIC unit
3.) TIC Gas Type Configuration
   a) Navigate to the Pressure Indication menu on TIC
   b) Enter the Gas Type settings:
      i) Select Nitrogen for general vacuum tests
      ii) If the inner gas is $CO_2$, select $CO_2$
4.) ESAM Software Initialization
   a) Launch the ESAM software on PC
   b) Create a new test and select appropriate configuration
5.) Powering the HI
   a) Turn on the HI power source
   b) **Important**: Do not turn on the CI power source before the test, as it lacks output control and will begin regulation immediately

**Final Checks**

At the end of this setup, verify the following:

- HI and CI target temperature settings are correctly displayed on the temperature regulators
- Input voltage and current settings are visible on the HI power source
- ESAM software displays temperature data, pressure readings and HF information (if available)
- TIC display shows the TVAC internal pressure

## 4.7 Post-test Checklist

This procedure assumes that the test was conducted on TVAC, and the subsystems are in the following state:

- CI power source is off
- HI power source is off
- ESAM SW has completed data writing

- Vacuum pump is not running – if the tests were conducted at negative temperatures, turn off the vacuum pump after reaching at least 0 °C (to prevent formation of ice layer on specimen)

**ESAM Software Data Handling**

1.) Data Calibration
   a) Once data acquisition is completed, the ESAM SW will display a Data Calibration window
   b) Select "Calibrate now" to process the data
2.) Exporting ESAM Data
   a) Navigate to the data download section (last window in ESAM SW)
   b) Check the test name
   c) Select the relevant events and channels for export ("Select all" is recommended)
   d) Choose the data output folder
   e) Export the data in .txt format
3.) Opening Test Data in Excel
   a) Open Microsoft Excel
   b) Go to File → Open → locate the exported .txt file (You may need to change the file type selection to "All files *.*")
   c) The Text Import Wizard will appear:
      i) Select "Delimited" and click Next
      ii) Check "Space" as the delimiter (uncheck all others), then click Next
      iii) The formatted data should now appear in the Excel sheet.
4.) Use the pre-prepared Evaluation Sheet to copy and analyze the test data

**System Shutdown**

1.) Powering Down the System
   a) Close ESAM SW (ensure all test data is calibrated, saved, or exported before closing)
   b) Turn off TIC on the vacuum pumping station
   c) Shut down ESAM SW completely
   d) Disconnect the CI and HI temperature regulators from the power network
   e) Disconnect the ESAM power source from the power network
   f) Unplug the HI/CI power source heating resistors inputs
   g) Disconnect the HI and CI power sources from the power network
2.) TVAC Tightness Check
   a) Conduct a final check of the TVAC system's tightness to ensure it is properly sealed

# 5 Test Plan

The test plan defines the set of experimental procedures designed to fulfill the objectives of this thesis. The plan includes both cyclic and thermal balance tests conducted in vacuum and $CO_2$ atmosphere using different specimens.

**Phase 1 (Pilot Tests)**

Pilot tests were conducted initially in the process of developing testing procedures, prior to the main test campaign. Its primary role was to establish whether the TVAC and all other equipment ($CO_2$ supply system, LIN feed, DAS…) were functional as well as determine whether stable and repeatable measurements were possible within the thermal vacuum chamber. These tests played a significant role in all the other experiments, including the cyclic tests and the thermal balance tests.

**Phase 2 (Cyclic Tests)**

In this phase of test campaign, two preliminary feasibility tests were conducted, where adjustments (change of power input, temperature gradient…) were made. Then, one full cyclic test in vacuum and one full cyclic test in CO2 atmosphere were executed.

**Phase 3 (Thermal Balance Tests)**

The Table 5.1 shows the "envelope" of the conducted regulated tests with aluminium dummy (Al 7075 T73). Based on Chapter 4.2 (second paragraph of thermal balance test discussing overly high temperatures on HI) and limiting operating temperatures of some components (described in Table 2.2), unregulated thermal balance tests were conducted only with input power of 2, 4 and 6 W. Due to the same reason, regulated test with input power of 10 W and temperature on cold interface equal to 30 °C was not conducted.

*Table 5.1 Test envelope for thermal balance tests (regulated)*

| Thermal Balance Tests (Regulated) | | | | |
|---|---|---|---|---|
| | Input Power (W) | | | |
| Temp. on CI (°C) | 2 | 4 | 7 | 10 |
| -15 | ✓ | | | ✓ |
| 0 | | | | |
| 15 | | | | ✓ |
| 30 | ✓ | | ✓ | |

**Test Overview**

This chapter provides an overview of the test plan (Table 5.2), broken down to three main phases. Phase 1, as an initial phase, where pilot tests were conducted. Phase 2 for the cyclic

tests (in vacuum and in $CO_2$ atmosphere), and Phase 3 for the thermal balance tests with aluminium specimen.

*Table 5.2 Test overview*

| Test Name | TVAC Config. | Specimen | Event | Regulation | Power | CI Temp. | Env. |
|---|---|---|---|---|---|---|---|
| | | | | Yes/No | [W] | [°C] | Vac/$CO_2$ |
| **PHASE 1 (Pilot Tests)** | | | | | | | |
| 1000 | 1B | Bronze Dummy | 1 | Yes | 4 | -15 | CO2 |
| 1001 | 1B | Bronze Dummy | 1 | No | 4 | - | Vac |
| 1001 | 1B | Bronze Dummy | 2 | No | 4 | - | Vac |
| 1002 | 1B | Bronze Dummy | 1 | Yes | 4 | 0 | Vac |
| 1002 | 1B | Bronze Dummy | 2 | Yes | 4 | -15 | Vac |
| 1002 | 1B | Bronze Dummy | 3 | Yes | 4 | 30 | Vac |
| **PHASE 2 (Cyclic Tests)** | | | | | | | |
| 1003 | 2 | Bronze Dummy | 1 | Yes | 4 | - | Vac |
| 1003 | 2 | Bronze Dummy | 2 | Yes | 10 | - | Vac |
| 1004 | 2 | Bronze Dummy | 1 | Yes | 97 | - | Vac |
| 1005 | 2 | Bronze Dummy | 1 | Yes | 97 | - | CO2 |
| **PHASE 3 (Thermal Balance Tests)** | | | | | | | |
| 1006 | 1B | Al Dummy | 1 | No | 2 | - | Vac |
| 1007 | 1B | Al Dummy | 1 | No | 4 | - | Vac |
| 1007 | 1B | Al Dummy | 2 | No | 4 | - | Vac |
| 1008 | 1B | Al Dummy | 1 | No | 6 | - | Vac |
| 1008 | 1B | Al Dummy | 2 | No | 6 | - | Vac |
| 1009 | 1B | Al Dummy | 1 | Yes | 2 | -15 | Vac |
| 1009 | 1B | Al Dummy | 2 | Yes | 2 | 30 | Vac |
| 1010 | 1B | Al Dummy | 1 | Yes | 7 | 30 | Vac |
| 1011 | 1B | Al Dummy | 1 | Yes | 10 | -15 | Vac |
| 1011 | 1B | Al Dummy | 2 | Yes | 10 | 15 | Vac |

# 6 Results & Test Procedures

## 6.1 Pilot Test Experiment in CO2 Atmosphere

**Test Setup**

| | |
|---|---|
| Test facility | TVAC Version 3 |
| Specimen | Bronze ($CuSn_8$) Dummy |
| Inner gas | $CO_2$ |
| Inner pressure | ≈1000 Pa |
| HI input power | 4 W |
| CI constant temperature | -15 °C |
| TVAC Configuration | 1b |
| WRG position | Bottom |
| Weight | Yes |
| Copper belts | No |
| Regulators | HI: Yes<br>CI: Yes |
| HF sensor | Yes (between HI and HCP) |
| Thermocouples | 5x HCP (TH2, TH3, TH4, TH6, TH7)<br>5x CCP (TC2, TC3, TC4, TC6, TC7)<br>1x CI (TC8)<br>1x HI (TH8)<br>1x inner TVAC wall (TC1)<br>3x outer (TO1, TO2, TO3) |

**Test Procedure**

This test assumes that all systems have been connected and powered on as described in Chapter 4.6.

1.) Set Temperature on CI Regulator
   a) Adjust the CI temperature regulator to the intended CCP temperature (=-15 °C)
2.) Configure HI Power Source
   a) Set the input voltage and current based on the required heat load (=4 W) for the test
3.) Verify TIC Gas Settings
   a) Ensure the TIC gas type is set to Nitrogen ($N_2$)
4.) Enable Vacuum Pump Gas Ballast
   a) Move the Gas Ballast knob on the vacuum pump to the ON position (open "|")
5.) Start Data Acquisition in ESAM SW
   a) Select "Begin Acquisition"
   b) Click "Start Writing" to log test data
6.) Begin TVAC Evacuation
   a) In the TIC menu, activate the vacuum system by selecting "Cycle On"
7.) Set HI Temperature Regulator
   a) Adjust the HI temperature regulator to 100 °C (this setting will ensure a constant heat load throughout the test

8.) Move Gas Ballast knob after Initial Evacuation
    a) After 16 hours of evacuation, move the Gas Ballast knob on the vacuum pump to the OFF position (closed "O")
9.) Change TIC Gas Settings
    a) Ensure the TIC gas type is set to carbon dioxide ($CO_2$)
10.) Introduce $CO_2$ into TVAC Chamber
    a) Open the Reduction valve on the $CO_2$ tank
    b) Open the Leak valve on TVAC and adjust to set the pressure in TVAC to 1000 Pa
    c) Close the Leak valve
    d) Close the Reduction valve
11.) Activate HI Power Source Output
    a) Press the "Output" button on the HI power source to start power delivery
12.) Power on CI System
    a) Turn on the CI power source
13.) Start Manual Cooling Procedure
    a) Pour liquid nitrogen (LIN) into the CI LIN tank when the CI temperature exceeds the intended CCP temperature as defined by test parameters
    b) Monitor the CCP temperature drop to ensure proper cooling
14.) Maintain CCP Temperature
    a) Repeat step 13 as needed to keep the CCP temperature stable
15.) Reach Steady-state Conditions
    a) Follow the steady-state criteria outlined in Chapter 2.4
16.) Record Steady-state Data
    a) Maintain steady-state conditions for at least 60 minutes
    b) Ensure that steady-state conditions have been met for the last hour of measurement
17.) Turn Off CI Power Source
18.) Turn Off HI Power Source Output
19.) Stop Data Acquisition in ESAM SW
    a) Select "Stop Writing" and "Stop Acquisition" in ESAM software to finalize data recording

**Results and Observations**

The Pilot Test in $CO_2$ atmosphere was conducted to verify the stability of the test environment and to identify potential issues in data acquisition. The required pressure of 1000 Pa for the test was achieved (Figure 6.1). At the end of evacuation, the pressure reached value less than $2 \cdot 10^{-4}$ Pa. After reaching the steady state in $CO_2$ atmosphere, the average pressure was 1034.16 Pa, with pressure difference ±0.155 %.

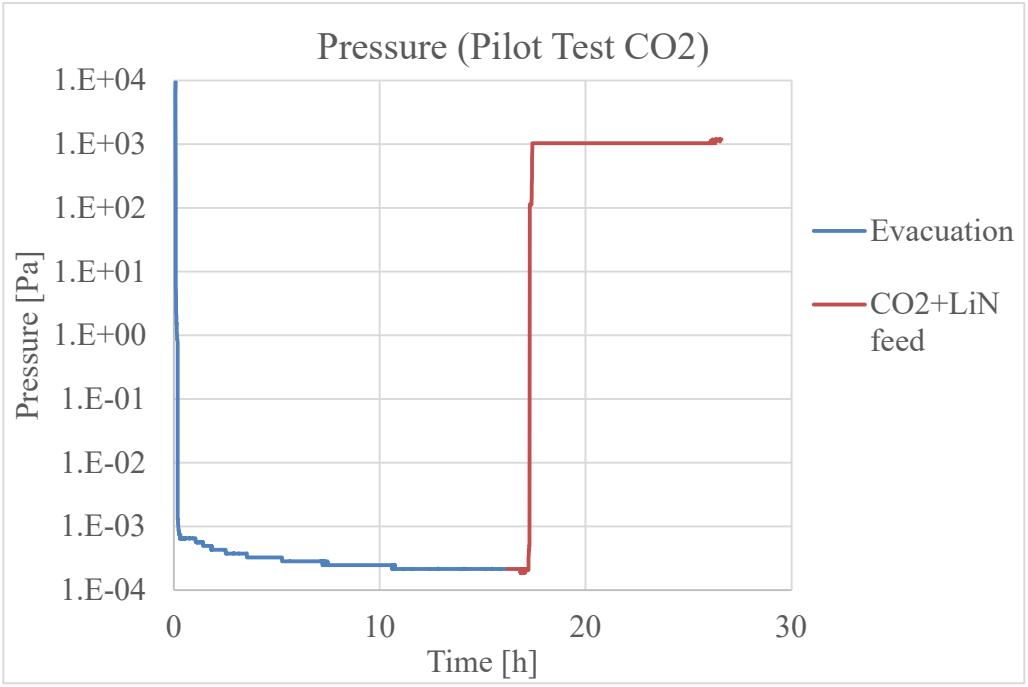


*Figure 6.1 Pressure in TVAC during pilot test*

A steady state was achieved in 1.7 hours (Figure 6.2). The required temperature on CI during the steady state for the Pilot test in $CO_2$ atmosphere was -15 °C, with maximum deviation of ±0.5 °C. The correct temperature regulation was achieved 86.9% of the time.

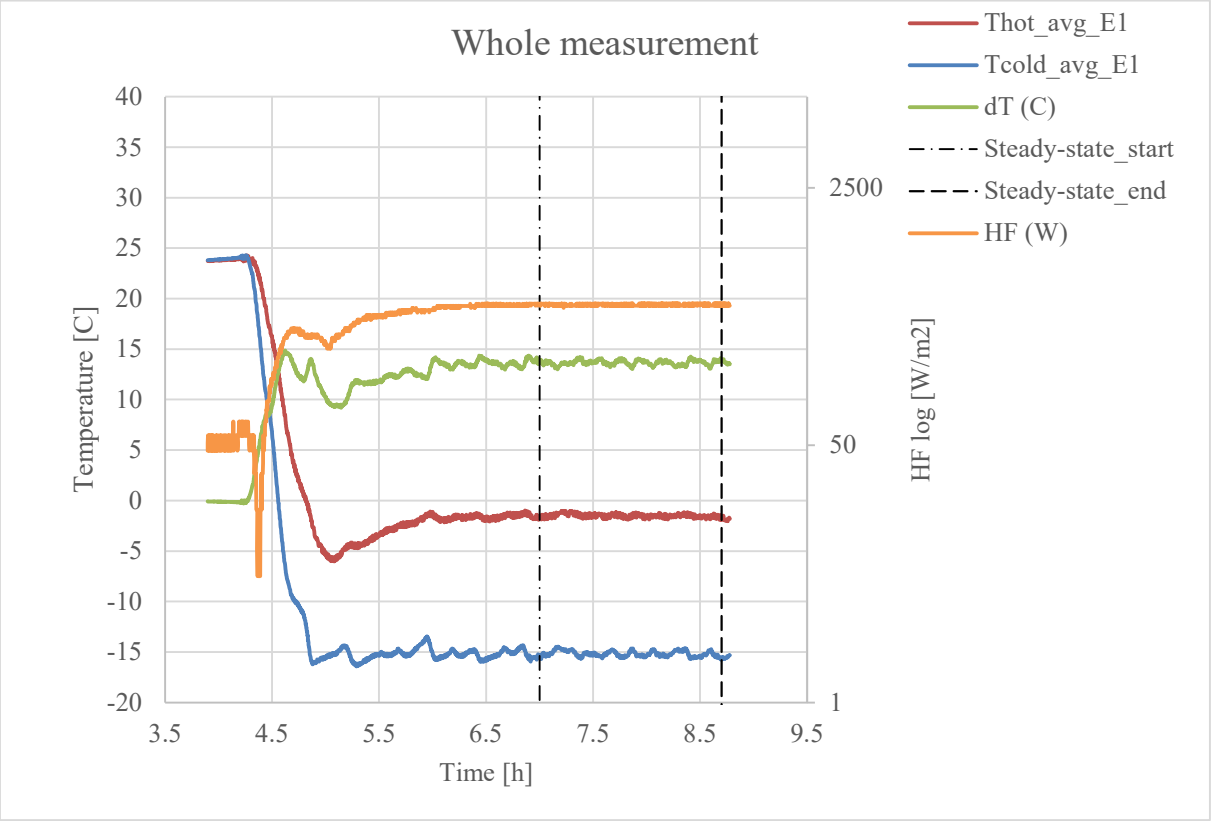


*Figure 6.2 Pilot test ($CO_2$ atmosphere)*

In the Pilot Test ($CO_2$ atmosphere), heat flux readings showed an oscillation in recorded values (Figure 6.3). The fluctuations ranged from -4.41 to 1.93 % around the average value of 423,7 W/m$^2$, which can be considered a stable heat flux reading.

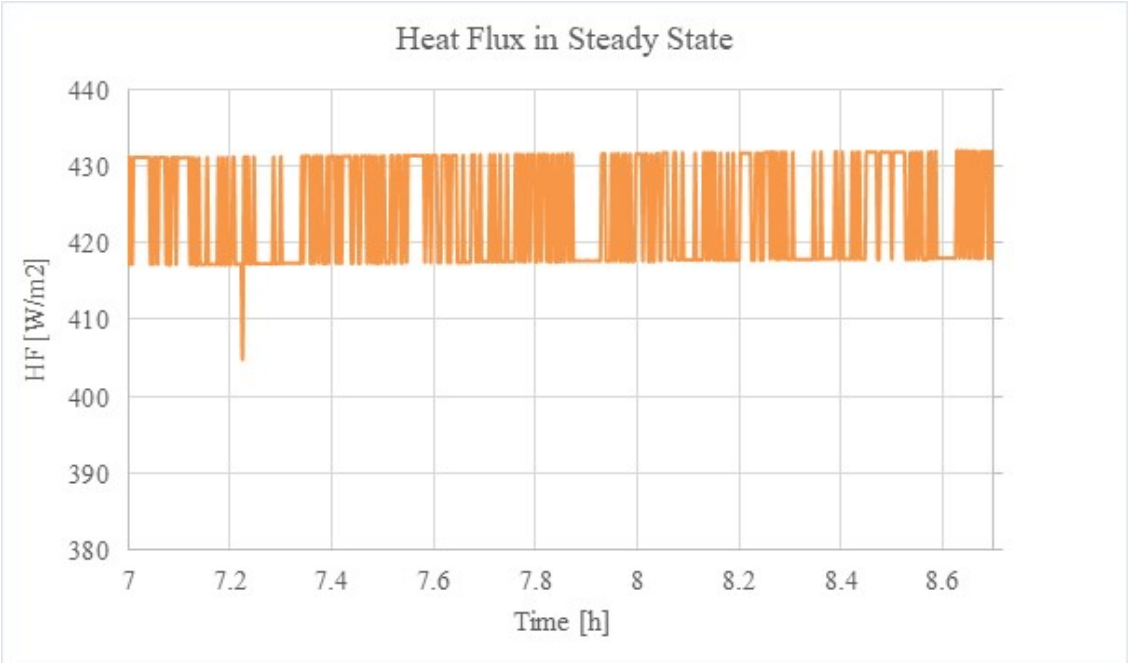


*Figure 6.3 Heat flux fluctuations*

## 6.2 Pilot Test Experiments in Vacuum

**Test Setup**

| | |
|---|---|
| Test facility | TVAC Version 3 |
| Specimen | Bronze ($CuSn_8$) Dummy |
| Inner gas | $N_2$ (Vacuum) |
| Inner pressure | $<10^{-3}$ Pa |
| HI input power | 4 W |
| CI constant temperature | -15 °C, 0 °C, 30 °C |
| TVAC Configuration | 1b |
| WRG position | Bottom |
| Weight | Yes |
| Copper belts | No |
| Regulators | HI: Yes<br>CI: Yes |
| HF sensor | Yes (between HI and HCP) |
| Thermocouples | 5x HCP (TH2, TH3, TH4, TH6, TH7)<br>5x CCP (TC2, TC3, TC4, TC6, TC7)<br>1x CI (TC8)<br>1x HI (TH8)<br>1x inner TVAC wall (TC1)<br>3x outer (TO1, TO2, TO3) |

**Test Procedure**

This test assumes that all systems have been connected and powered on as described in Chapter 4.6.

1.) Set Temperature on CI Regulator
   a) Adjust the CI temperature regulator to the intended CCP temperature
2.) Configure HI Power Source
   a) Set the input voltage and current based on the required heat load (=4 W) for the test
3.) Verify TIC Gas Settings
   a) Ensure the TIC gas type is set to Nitrogen ($N_2$)
4.) Enable Vacuum Pump Gas Ballast
   a) Move the Gas Ballast knob on the vacuum pump to the ON position (open "|")
5.) Start Data Acquisition in ESAM SW
   a) Select "Begin Acquisition"
   b) Click "Start Writing" to log test data
6.) Begin TVAC Evacuation
   a) In the TIC menu, activate the vacuum system by selecting "Cycle On"
7.) Set HI Temperature Regulator
   a) Adjust the HI temperature regulator to 100 °C (this setting will ensure a constant heat load throughout the test
8.) Change TIC Gas Settings
   a) Ensure the TIC gas type is set to carbon dioxide ($CO_2$)

9.) Activate HI Power Source Output
   a) Press the “Output” button on the HI power source to start power delivery
10.) Power on CI System
   a) Turn on the CI power source
11.) Start Manual Cooling Procedure
   a) Pour liquid nitrogen (LIN) into the CI LIN tank when the CI temperature exceeds the intended CCP temperature as defined by test parameters
   b) Monitor the CCP temperature drop to ensure proper cooling
12.) Maintain CCP Temperature
   a) Repeat step 11 as needed to keep the CCP temperature stable
13.) Reach Steady-state Conditions
   a) Follow the steady-state criteria outlined in Chapter 2.4
14.) Record Steady-state Data
   a) Maintain steady-state conditions for at least 60 minutes
   b) Ensure that steady-state conditions have been met for the last hour of measurement
15.) Turn Off CI Power Source
16.) Turn Off HI Power Source Output
17.) Stop Data Acquisition in ESAM SW
   a) Select “Stop Writing” and “Stop Acquisition” in ESAM software to finalize data recording

**Results and Observations**

In Table 6.1 are the test results of the initial tests with bronze dummy. The test with $CO_2$, compared to vacuum test at same CI temperature (test 1002 Event 1 & 2, where pressure values were in ten thousandths Pa range) shows a decrease of heat flux by 61.5 %, total resistance increase by 65.5 % and thermal contact conductivity decrease by 43.7 %. One contributing factor is that at -15 °C the thermal conductivity of $CO_2$ is slightly smaller than that of air [19, p. 5]. Also, at 1000 Pa, $CO_2$ is in low-pressure regime, where the mean free path of the molecules is quite large and they do not collide too often to transfer significant heat, hence the decrease of heat flux. In vacuum tests, heat transfer occurs almost exclusively through Dummy and gas-phase conduction is negligible, resulting in higher thermal resistance.

The two unregulated tests (1001 Event 1 & 3) were conducted under almost the same conditions, only in test 1001, the temperature of the environment surrounding the TVAC was slightly lower. The average heat flux recorded was 1119.35 W/m2 (±4.8 %), average total resistance was 6,569 K/W (±5.74 %) and average thermal contact conductance for based on previous experiments for bronze dummy with thermal conductance of specimen equal to 0.744 $W/m^2 \cdot K$ and surface area of $2259 \cdot 10^{-6}$ $m^2$ was 236.53 $W/m^2 \cdot K$ (±7.21 %).

The rest of the tests were regulated with liquid nitrogen, to have stable temperature on cold interface throughout the whole test. Figure 6.4 shows the heat flux and temperature difference between HI and CI based on the temperature on CI during testing. The heat flux almost does not change throughout different tests with different settings. The difference is only -1.88 %.

Total resistance also decreases with higher temperatures on CI, while thermal contact conductance increases (Figure 6.5). The temperature difference is directly affected by the total thermal resistance and the heat flow. Lower total resistance leads to a smaller temperature difference between hot and cold interface based on Fourier's law based on the analogy of Ohm's law. (Eq. (6.2)).

$$R = \frac{dT}{Q_{in}} \tag{6.1}$$

*Table 6.1 Test results (initial tests)*

| Test Number | Event | Regulated | Qin | Tcold | dT | HF | Qin (HF) | Rtot | TCR | TCCvac |
|---|---|---|---|---|---|---|---|---|---|---|
| [-] | [-] | [-] | [W] | [°C] | [°C] | [W/m^2] | [W] | [K/W] | [K/W] | [W/m^2*K] |
| 1000 | 1 | Yes | 4 | -15.16 | 13.67 | 423.7 | 0.96 | 14.28 | 6.47 | 95.05 |
| 1001 | 1 | No | 4 | 38.18 | 16.41 | 1173.1 | 2.65 | 6.19 | 2.42 | 253.58 |
| 1001 | 2 | No | 4 | 40.69 | 16.72 | 1065.6 | 2.41 | 6.95 | 2.80 | 219.47 |
| 1002 | 1 | Yes | 4 | -14.95 | 21.46 | 1101.0 | 2.49 | 8.63 | 3.64 | 168.75 |
| 1002 | 2 | Yes | 4 | 0 | 19.90 | 1114.5 | 2.52 | 7.90 | 3.28 | 187.45 |
| 1002 | 3 | Yes | 4 | 30.12 | 17.71 | 1093.5 | 2.47 | 7.17 | 2.91 | 210.99 |

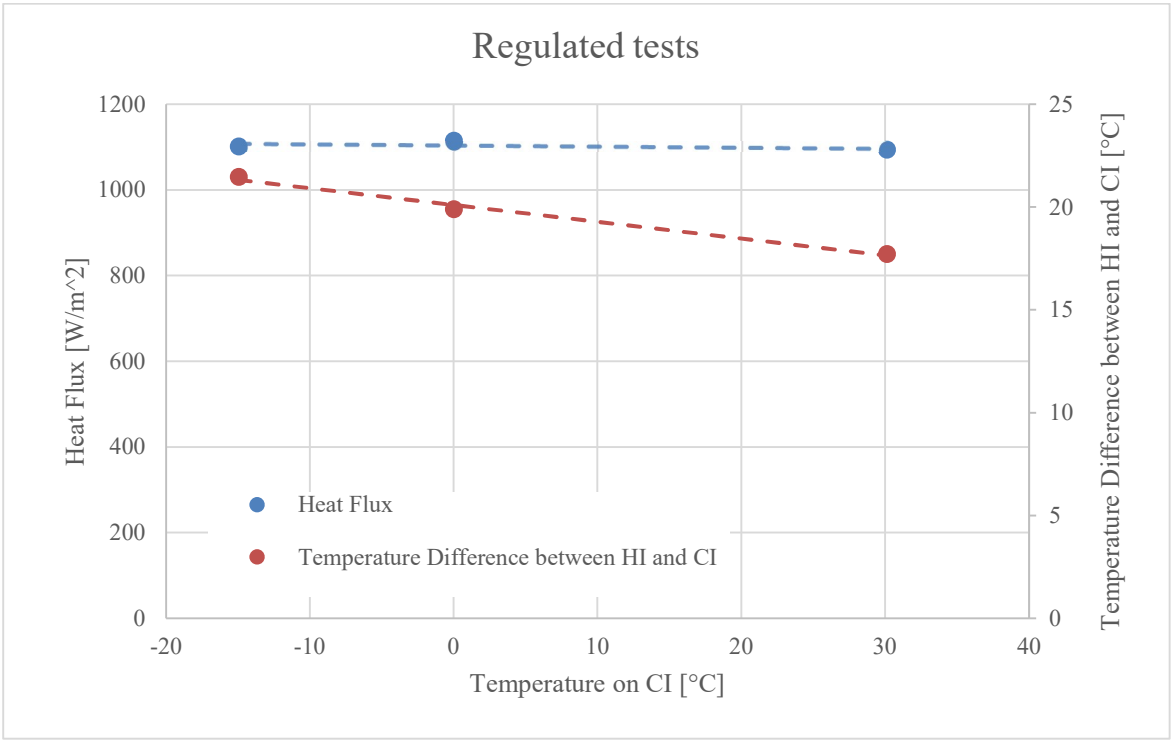


*Figure 6.4 Regulated pilot tests results (1)*

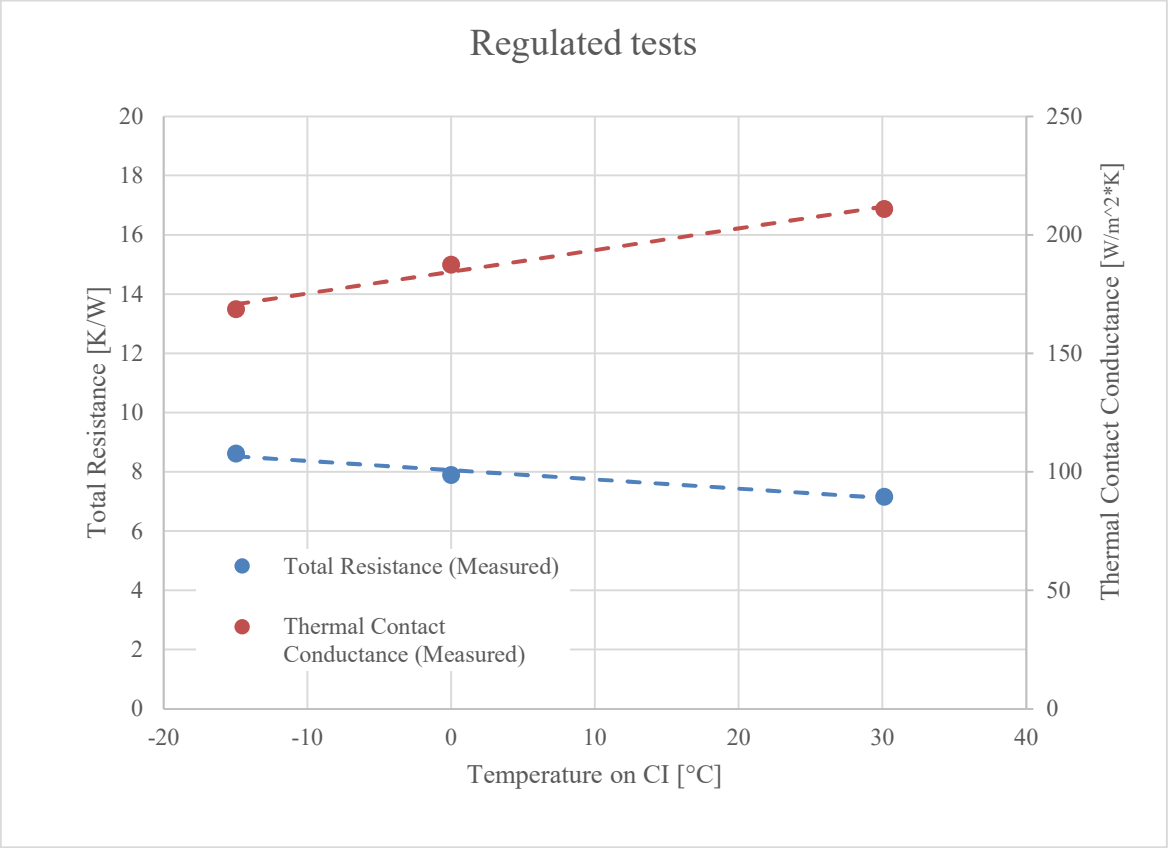


*Figure 6.5 Regulated pilot tests results (2)*

For comparison, a measurement that was conducted in 2021 at IAE with a CuSn8 specimen can be seen in Figure 6.6. The measurement was performed at 20 °C and 60 °C and values for thermal conductivity of CuSn8 were found. Thermal contact conductance values were calculated using CFD simulation of the dummy. To find values for other temperatures, ranging from -30 °C to 60 °C, linear approximation was used. To compare the values, equation (6.2) was used(6.2), where the left side of the equation is total resistance measured in 2025 and the left side of the equation are values acquired in measurement from 2021 (first equation term is resistance of specimen at average temperature divided by 1.5 to match with current test configuration, second term is thermal contact resistance at cold interface temperature and third term is thermal contact resistance at hot interface temperature). The declining trend of total resistance with higher temperatures on CI is similar at both measurements. The difference between measurements at positive temperatures is within range of 6 % (see Table 6.2). At negative temperatures, the difference is higher, which can be caused by using the linear approximation (of only two positive temperatures) for 2021 measurement data. Also, the measurement of new data (from 2025) introduces some error in final values of total resistance.

$$\frac{\Delta T}{Q_{in}} = R_{TOT} = R_{SPEC}\left(T_{AVG} = \frac{T_{HI} - T_{CI}}{2}\right) + TCR_1\,(T_{CI}) + TCR_2\,(T_{HI}) \qquad (6.2)$$

*Table 6.2 Values of total resistance - comparison*

| Temperature on CI [°C] | $R_{tot}$ (2021) [K/W] | $R_{tot}$ (2025) [K/W] | % [-] |
|---|---|---|---|
| -15 | 7.474 | 8.629 | 11.79 |
| 0 | 7.719 | 7.903 | 5.73 |
| 30 | 7.036 | 7.171 | 1.92 |

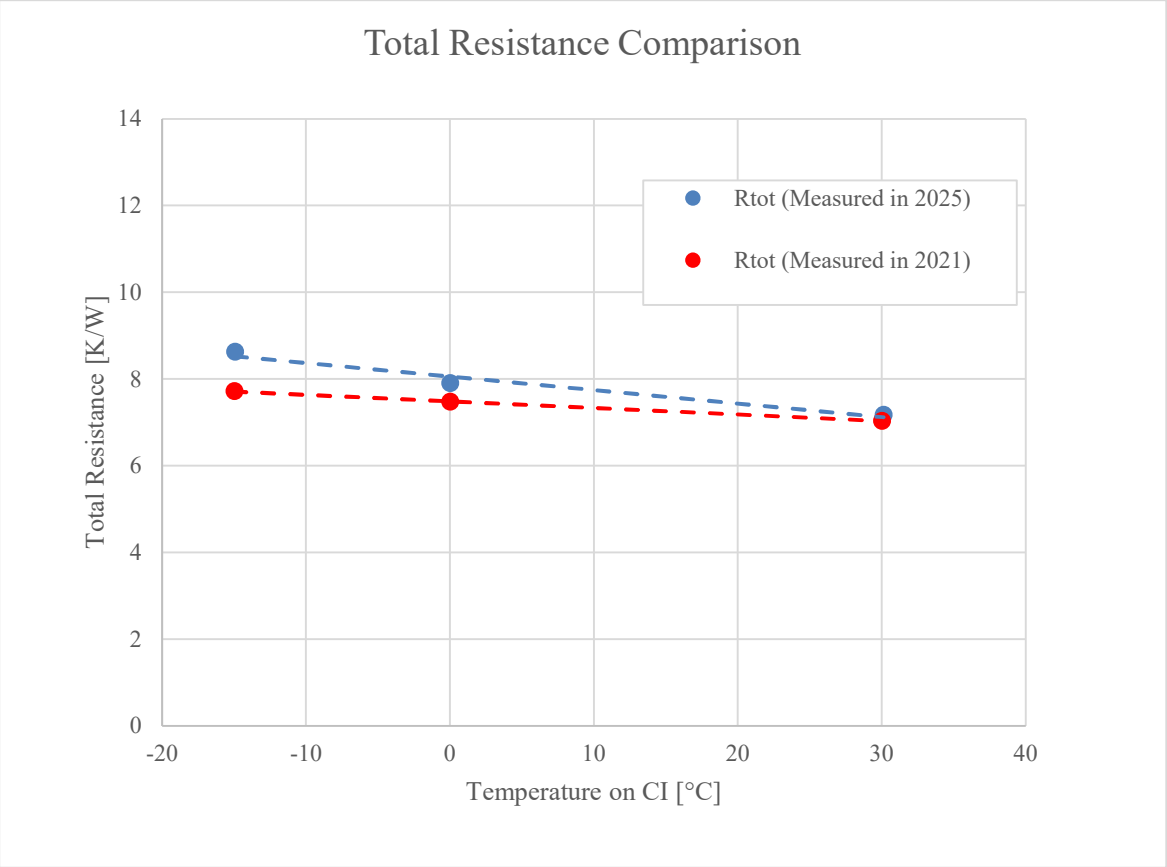


*Figure 6.6 Comparison with 2021 measurement (total resistance)*

## 6.3 Cyclic Test Experiments

**Test Setup**

| | |
|---|---|
| Test facility | TVAC Version 3 |
| Specimen | Bronze ($CuSn_8$) Dummy |
| Inner gas | $N_2$ (Vacuum) / $CO_2$ |
| Inner pressure | $<10^{-3}$ Pa (for vacuum test) / ≈1000 Pa (for $CO_2$ test) |
| HI input power | 97 W |
| CI constant temperature | - |
| TVAC Configuration | 2 |

| | |
|---|---|
| WRG position | Bottom |
| Weight | Yes |
| Copper belts | Yes |
| Regulators | HI: Yes<br>CI: Yes |
| HF sensor | No |
| Thermocouples | 5x HCP (TH2, TH3, TH4, TH6, TH7)<br>5x CCP (TC2, TC3, TC4, TC6, TC7)<br>1x CI (TC8)<br>1x HI (TH8)<br>1x inner TVAC wall (TC1)<br>3x outer (TO1, TO2, TO3) |

**Test Procedure**

This test assumes that all systems have been connected and powered on as described in Chapter 4.6.

1.) Set up the program for both PID regulators based on the Chapter 2.3.1
   a) Program both regulators using programming menu. Step "SoAk" to stay at designed temperature, "StPt" for reaching final temperature at designated time and "End" to end the program
2.) Verify TIC Gas Settings
   a) Ensure the TIC gas type is set to Nitrogen ($N_2$) for vacuum test
   b) Ensure the TIC gas type is set to carbon dioxide ($CO_2$) for $CO_2$ test
3.) Prepare Vacuum Pump
   a) Move the gas ballast knob to the ON position (open "I")
4.) Start Data Acquisition
   a) Launch ESAM software, click "Begin Acquisition" and then "Start Writing"
5.) Evacuate Chamber
   a) In TIC menu select "Cycle On" to start vacuum pumping for 12 hours
6.) Create 1000 Pa $CO_2$ atmosphere (for the $CO_2$ test)
   a) Move the gas ballast knob to the OFF position (closed "O")
   b) Open the Reduction valve on the $CO_2$ tank
   c) Open the Leak valve on TVAC and adjust to set the pressure in TVAC to 1000 Pa
   d) Close the Leak valve
   e) Close the Reduction valve
7.) Turn On CI Power Source
8.) Configure HI Power Source for entire test
   a) Set a heat load of 90 W
   b) Press "Output" on the HI power source
9.) Begin Cold Cycle Cooling

a) Pour liquid nitrogen (LIN) into both CI and HI LIN tanks until temperature on HI regulator reaches -5 °C, then it is enough to pour LIN only in CI LIN tank, saving LIN for the entirety of the test
b) Monitor CCP temperature and adjust LIN input as needed
c) Continue cooling until target cold cycle temperatures are reached

10.) Maintain Cold Conditions
a) Ensure both HI and CI temperature regulators remain active
b) Maintain set temperatures for 60 minutes, repeating LIN filling as needed

11.) Hot Cycle Procedure
a) Monitor both HI and CI temperature values on regulators during heating
b) Maintain the set temperatures for 60 minutes

12.) Thermal Cycling Repetition
a) Repeat the steps 9–10 for cold cycle one more time
b) Repeat step 11 for hot cycle one more time

13.) Terminate Vacuum Operation
a) In TIC menu select “Cycle off” to stop evacuation

14.) Turn off Power Source
a) Power down CI power supply
b) Power down HI power supply

15.) Move the gas ballast knob to the ON position (open “I”) (for the $CO_2$ test)

16.) Stop Data Recording
a) In ESAM software, select “Stop writing” and ”Stop acquisition”

**Results and Observations**

It was decided that for the initial feasibility test, the heat flux sensor will be in the test setup. But after the test was conducted the data collected from the sensor showed no pattern for evaluation and future cyclic tests were conducted without it. But the sensor stayed in TVAC, because the cables leading from it to the pinout are connected with TH8 temperature sensor cables. Also, the initial temperature gradient that was chosen was problematic to maintain and the power input on HI power source was changed to 10 W.

The second feasibility test (Figure 6.7) shows that during the dwell time on maximum negative temperatures, the required temperature difference (-65 °C on HI and -135 °C on CI) could not be controlled. Also, the temperature on CI climbed much steeper and even surpassed the temperature on HI. For the future cyclic testing, the power input was raised to 97 W. Such high-power input can be allowed, because the power source is not sending the power the whole time, but only in impulses. Another finding from this test was that during the cooling, pour liquid nitrogen in both (HI and CI) LIN tanks at the same time, but when the temperature on HI reaches around 0 °C to -10 °C it is sufficient to pour liquid nitrogen only in CI LIN tank. Likewise during the dwell time at maximum negative temperatures. This measure helps lower the consumption of liquid nitrogen.

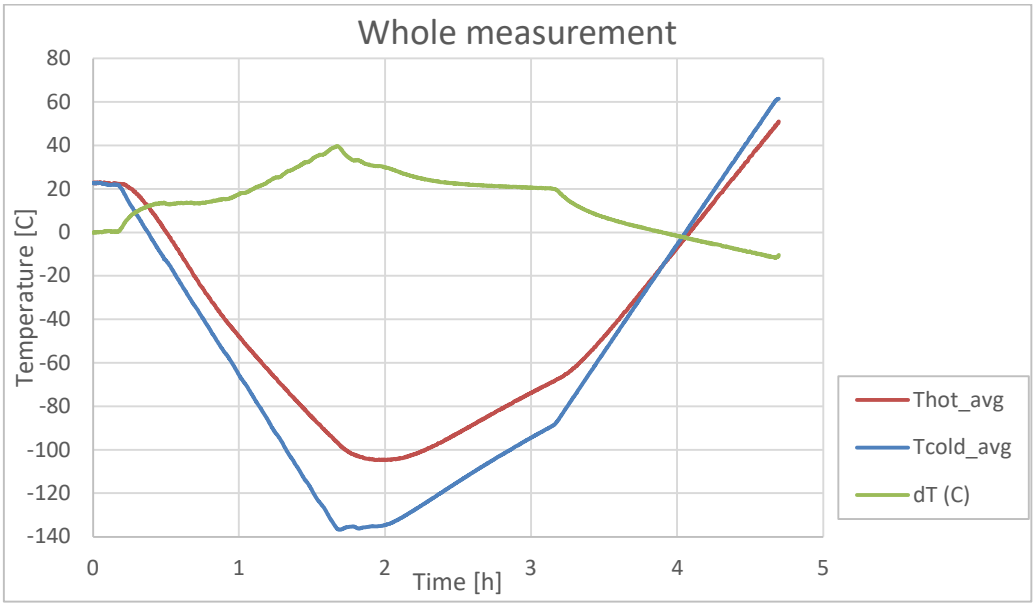


*Figure 6.7 Second feasibility test*

After gaining important experience from the feasibility tests first, the vacuum cyclic test was conducted. The temperature profiles in vacuum test (Figure 6.8) are almost similar to those mentioned in Chapter 2.3.1. Only during the dwell times, does the temperature slightly oscillate. "Thot_avg_prog" and "Tcold_avg_prog" are curves, that were programmed into the temperature regulators. The pressure during the vacuum test (Figure 6.9) develops as expected with temperature, where average value of pressure is $7.11 \cdot 10^{-5}$ Pa, maximal pressure $1.86 \cdot 10^{-4}$ Pa and minimal pressure is $2{,}05 \cdot 10^{-5}$ Pa.

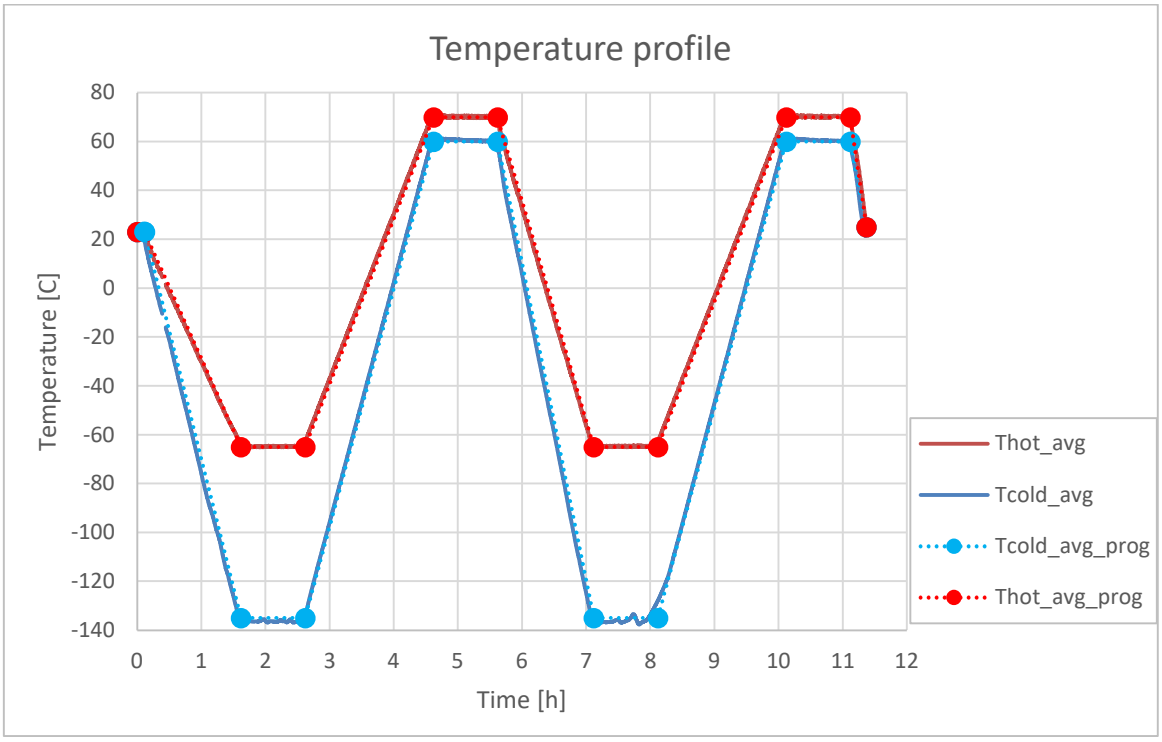


*Figure 6.8 Cyclic vacuum test*

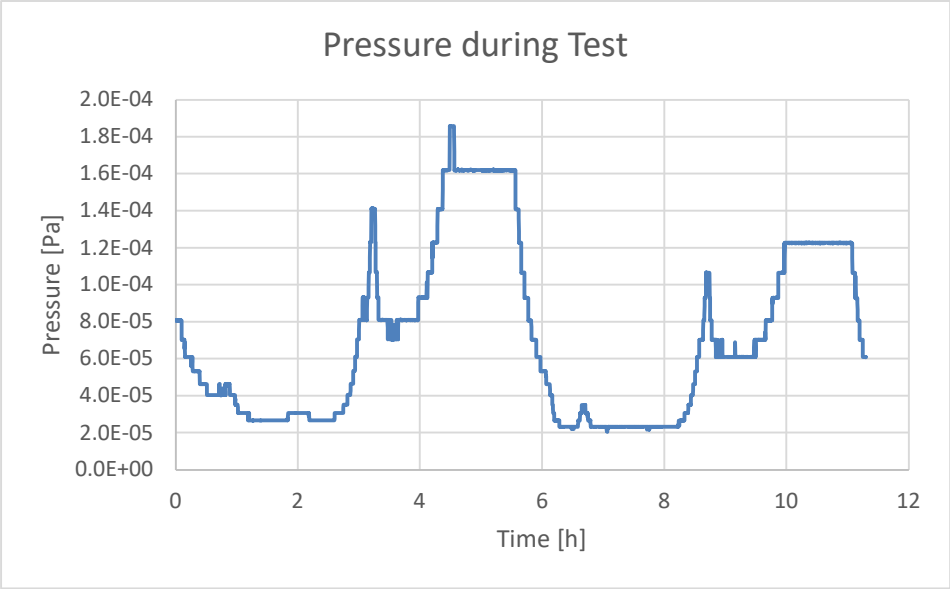


*Figure 6.9 Pressure in TVAC (vacuum cyclic test)*

The temperature profile for $CO_2$ cyclic test has slightly different gradients (Figure 6.10). They were changed so that they were the same when cooling and same during heating. The changed temperature profile was realized with no problems. The pressure was monitored on TIC menu, because of an issue with calibration in the TIC menu. The ESAM on PC was displaying pressure as if the TIC was calibrated for vacuum (Nitrogen) and TIC menu was displaying pressure correctly.

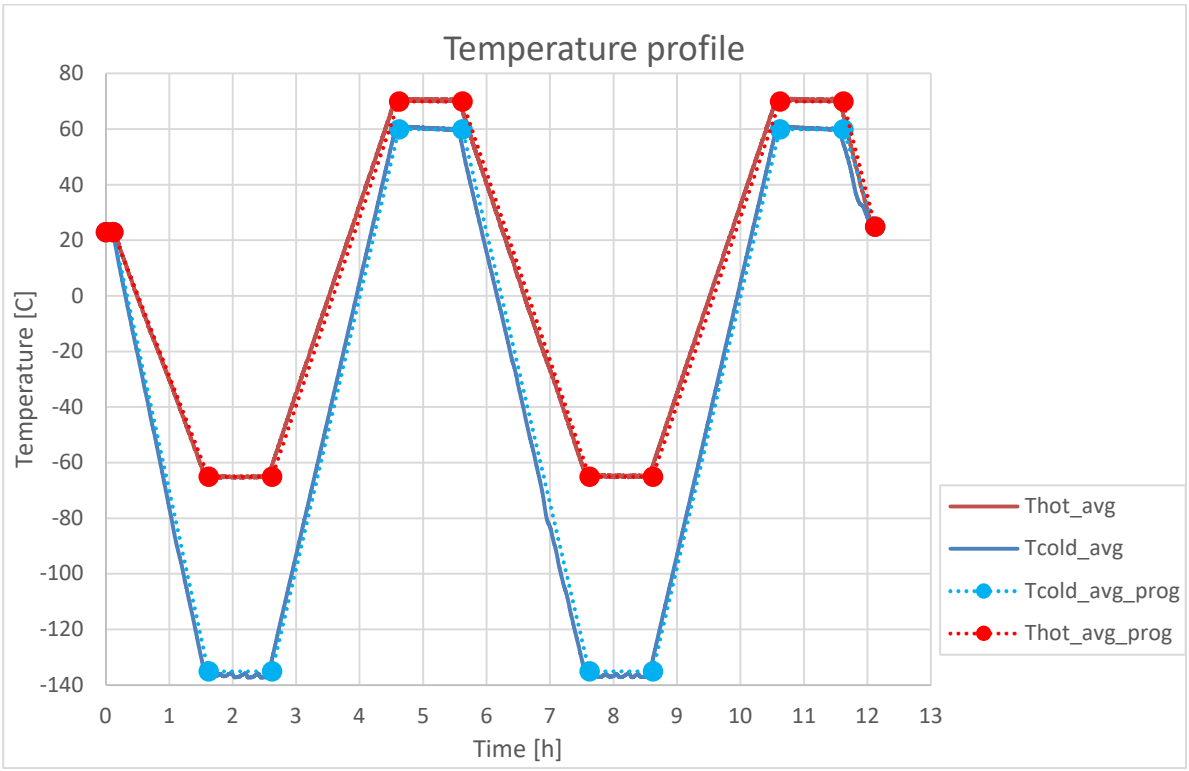


*Figure 6.10 Cyclic $CO_2$ test*

## 6.4 Thermal Balance Tests

**Test Setup**

| | |
|---|---|
| Test facility | TVAC Version 3 |
| Specimen | Aluminium (Al7075 T73) Dummy |
| Inner gas | $N_2$ (Vacuum) |
| Inner pressure | $<10^{-3}$ Pa |
| HI input power | 2, 4, 6 W (unregulated); 2, 7, 10 W (regulated) |
| CI constant temperature | -15 °C, 15 °C, 30 °C |
| TVAC Configuration | 1b |
| WRG position | Bottom |
| Weight | Yes |
| Copper belts | No |
| Regulators | HI: Yes<br>CI: Yes |
| HF sensor | Yes (between HI and HCP) |
| Thermocouples | 5x HCP (TH2, TH3, TH4, TH6, TH7)<br>5x CCP (TC2, TC3, TC4, TC6, TC7)<br>1x CI (TC8)<br>1x HI (TH8)<br>1x inner TVAC wall (TC1)<br>3x outer (TO1, TO2, TO3) |

**Test Procedure**

This test assumes that all systems have been connected and powered on as described in Chapter 4.6.

The test process follows the same steps as in pilot tests procedure, but with power input and CI temperatures regulation described in previous paragraph (Test Setup).

**Results and Observations**

Unregulated Tests

The results of unregulated tests with aluminium dummy can be seen in Table 6.3. The unregulated test with the same input power were always conducted twice, but results of one unregulated test with input power of 2 W appeared incorrect (e.g., triple the total resistance compared to the test with same input power). This test was removed from the test plan and the data collected from it are not considered in evaluation. The temperature (HI, CI and temperature difference) and pressure profiles can be seen in Figure 6.11. The pressure profiles have minimal oscillations, caused by ball valve 1, which was in open position throughout all the tests (turbo-pumping station was running constantly).

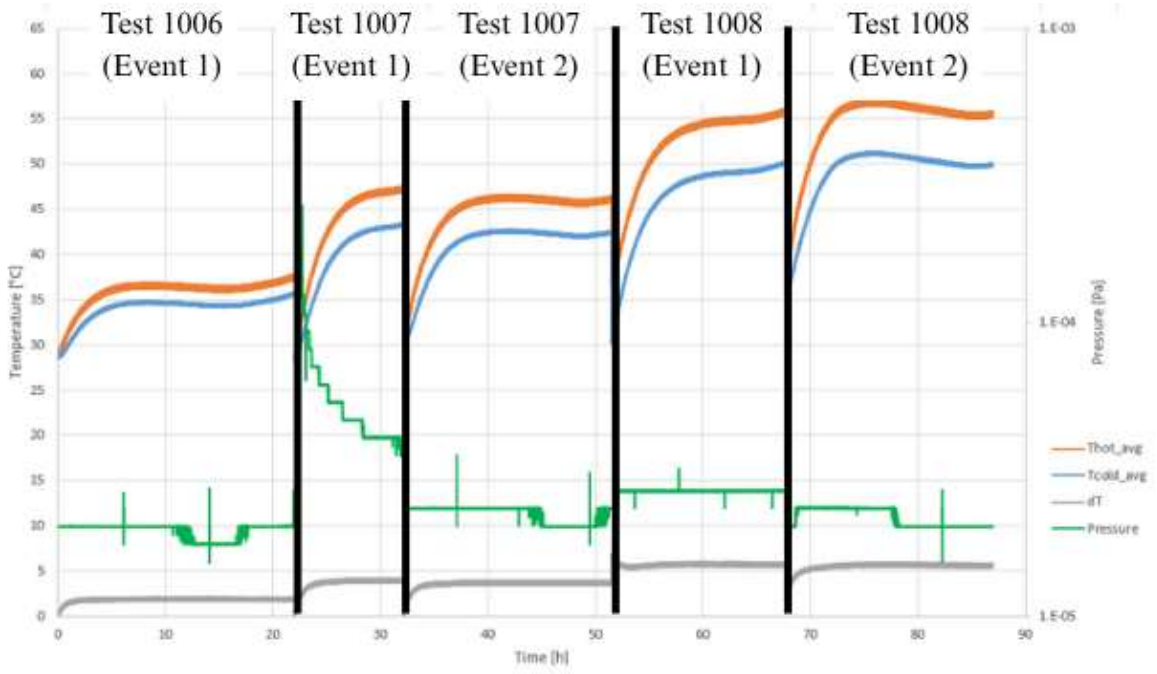


*Figure 6.11 Test profiles (unregulated tests)*

As can be seen in Table 6.3, all values for the tests with same input power are similar (the maximum difference is not higher than 5 %). For example the comparison for Test 1008: the heat flux in Event 1 is only 2.76 % higher than in Event 2 and the value of total resistance is 0.56 % smaller. Also, the similarity of values for total resistance and thermal contact resistance can be seen in Figure 6.12.

The average thermal contact resistance between aluminium and copper interfaces in unregulated tests is 0.52 K/W with a values ranging from -2.15 % to 3.9 %.

*Table 6.3 Unregulated tests (aluminium dummy)*

| Test Number | Event | Reg. | Qin | Tcold | dT | HF | Qin (HF) | Rtot | TCR | TCCvac |
|---|---|---|---|---|---|---|---|---|---|---|
| [-] | [-] | | [W] | [°C] | [°C] | [W/m^2] | [W] | [K/W] | [K/W] | [W/m^2*K] |
| 1006 | 1 | N | 2 | 34.5 | 1.87 | 672.85 | 1.52 | 1.23 | 0.607 | 862.55 |
| 1007 | 1 | N | 4 | 43.02 | 3.95 | 1590.35 | 3.59 | 1.10 | 0.541 | 967.79 |
| 1007 | 2 | N | 4 | 42.17 | 3.69 | 1547.11 | 3.49 | 1.06 | 0.520 | 1007.06 |
| 1008 | 1 | N | 6 | 49.07 | 5.72 | 2443.45 | 5.52 | 1.04 | 0.509 | 1027.69 |
| 1008 | 2 | N | 6 | 49.85 | 5.59 | 2376.13 | 5.37 | 1.04 | 0.512 | 1021.91 |

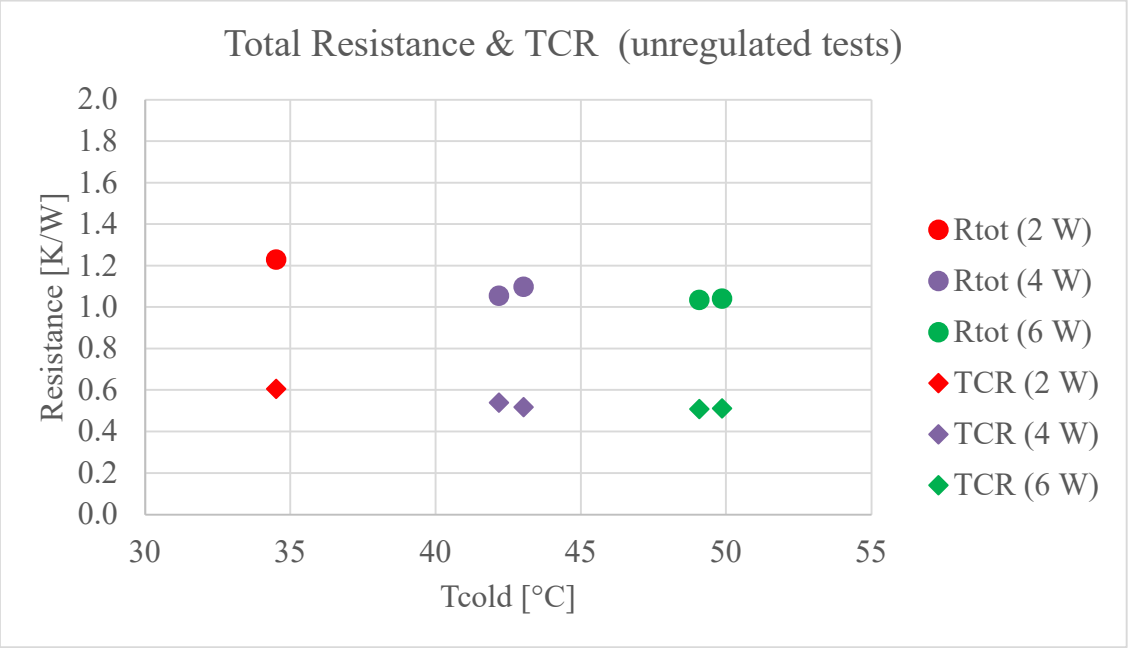


*Figure 6.12 Total resistance & TCR (unregulated tests)*

With increasing the power input, the heat flux, temperature on CI and temperature difference values are increasing (Figure 6.13). The total resistance and TCR values follow a decreasing trend with higher power inputs (Figure 6.12).

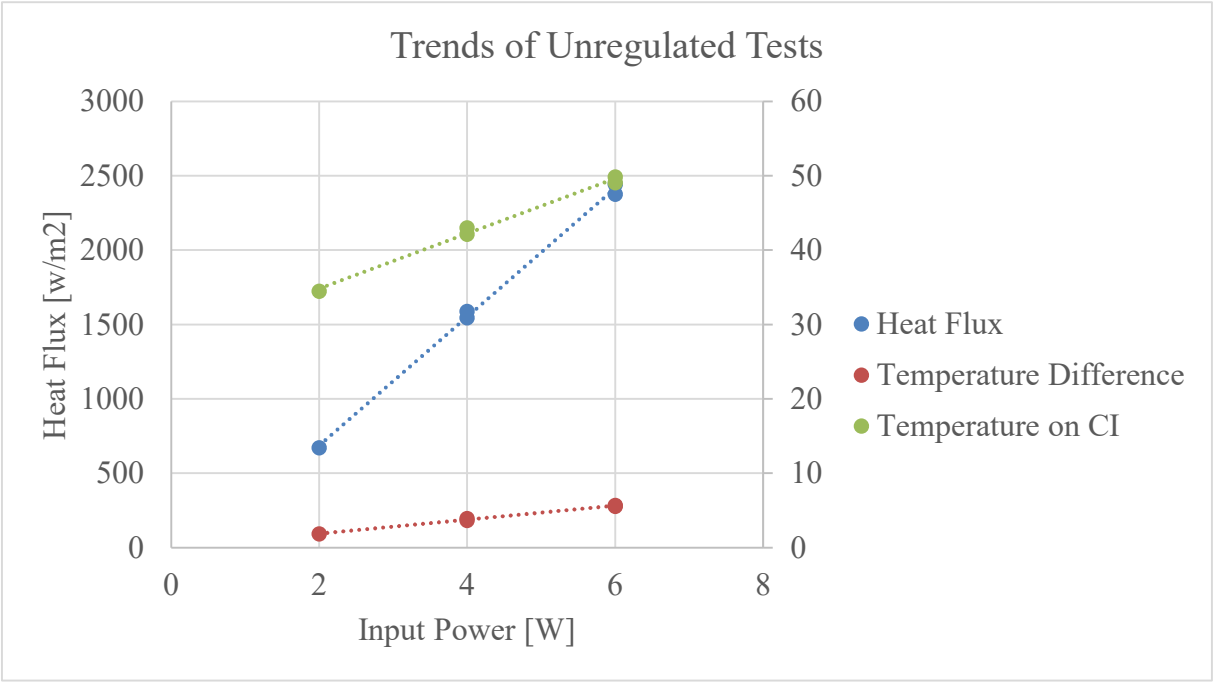


*Figure 6.13 Trends of unregulated tests*

Regulated Tests

As mentioned in Chapter 5, the regulated tests were conducted to create an envelope of boundary conditions that allows the evaluation of thermal contact performance across a range of heat loads. The acquired data from these tests can be seen in Table 6.4. The temperature (HI, CI and temperature difference) and pressure profiles can be seen in Figure 6.14. The heat flux values are similar for the same input power in all regulated tests (2W and 10W). As expected, increased power input results in a corresponding increase of the heat flux (Figure 6.15).

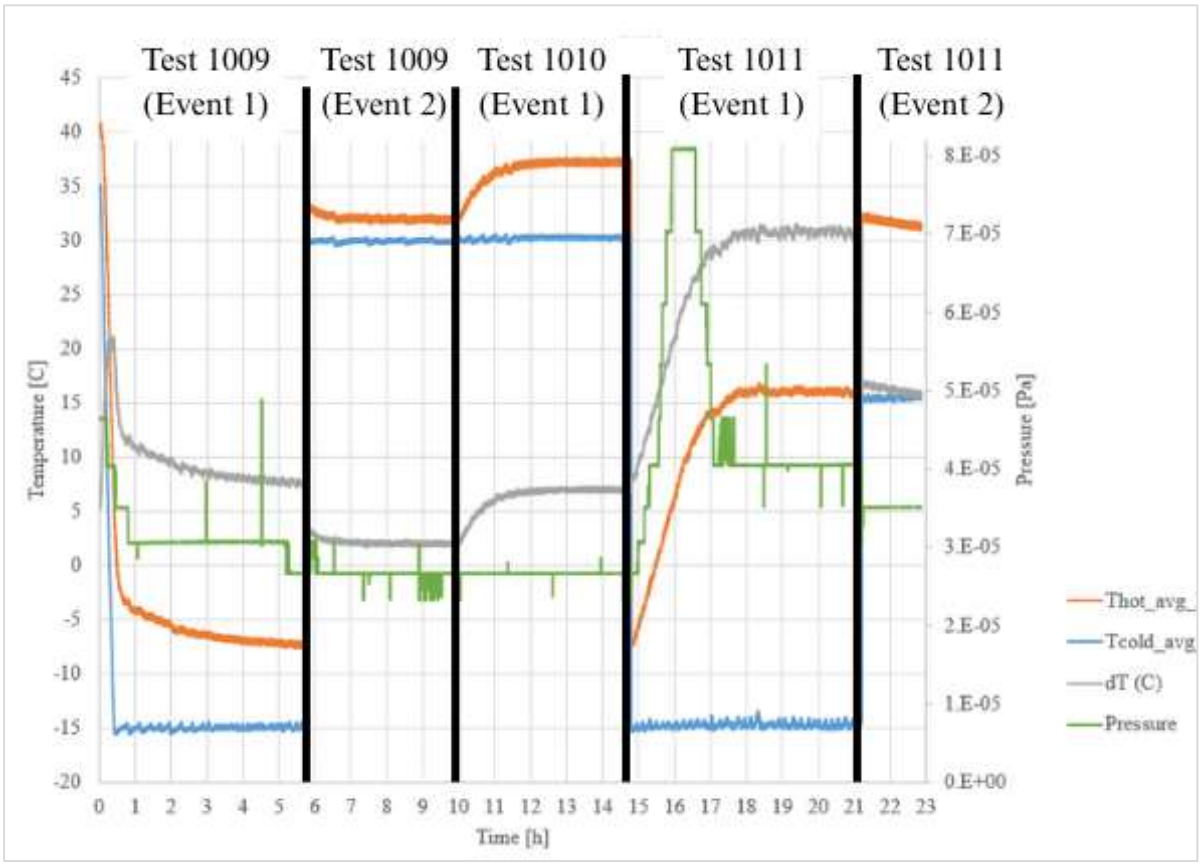


*Figure 6.14 Test profiles (regulated tests)*

Despite the identical power input, the total resistance, TCR and TCC values varied considerably across tests. This implies that mechanical and thermal stability of the contact interface may not have been fully consistent. An analysis of possible causes is presented in Chapter 7.

*Table 6.4 Regulated tests (aluminium dummy)*

| Test Number | Event | Reg. | Qin | Tcold | dT | HF | Qin (HF) | Rtot | TCR | TCCvac |
|---|---|---|---|---|---|---|---|---|---|---|
| [-] | [-] | | [W] | [°C] | [°C] | [W/m^2] | [W] | [K/W] | [K/W] | [W/m^2*K] |
| 1009 | 1 | Y | 2 | -14.94 | 7.85 | 688.49 | 1.56 | 5.05 | 2.515 | 208.00 |
| 1009 | 2 | Y | 2 | 29.92 | 2.02 | 728.90 | 1.65 | 1.23 | 0.606 | 863.91 |
| 1010 | 1 | Y | 7 | 30.234 | 6.97 | 2949.80 | 6.66 | 1.05 | 0.514 | 1017.97 |
| 1011 | 1 | Y | 10 | -14.71 | 30.75 | 4208.31 | 9.51 | 3.23 | 1.609 | 325.26 |
| 1011 | 2 | Y | 10 | 15.46 | 16.07 | 4201.60 | 9.49 | 1.69 | 0.838 | 624.41 |

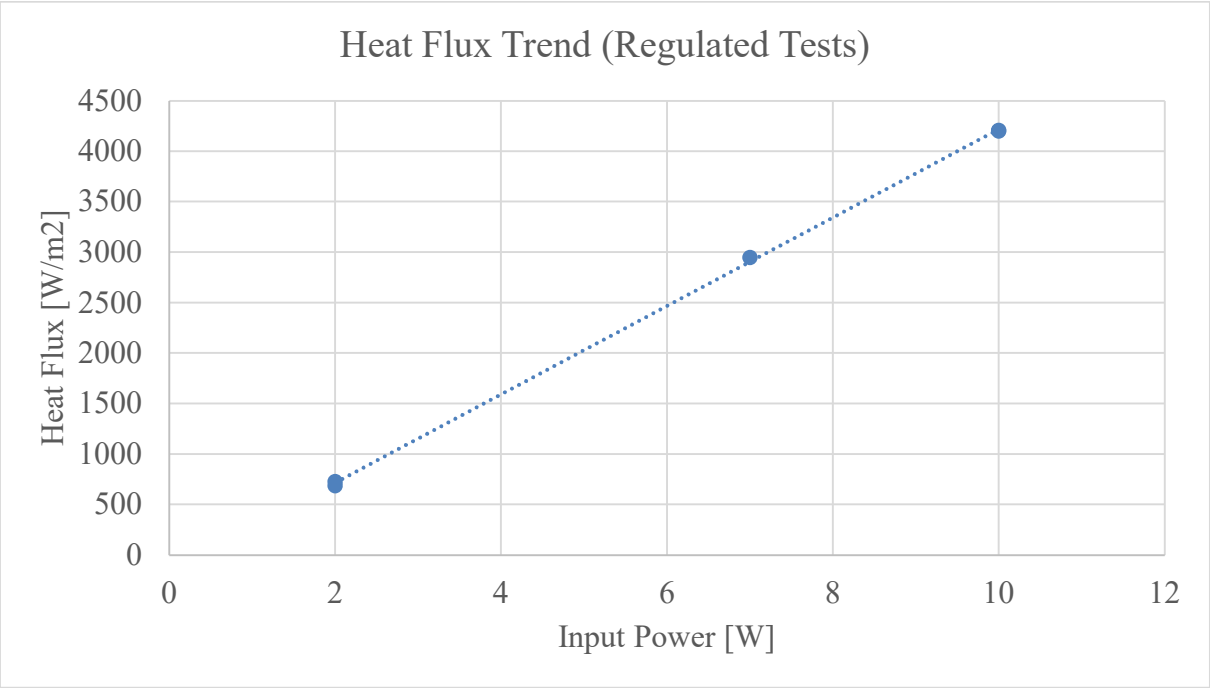


*Figure 6.15 Heat flux trend (regulated tests)*

# 7 Discussion

This chapter discusses important findings of the test campaign from irregular thermal contact resistance behavior to technical problems during cyclic testing. Detected issues (e.g., damaged cables) are discussed for future development. This chapter also outlines the next step in testing-changing the setup for evaluation of thermal parameters at aluminium-aluminium interface.

The cyclic tests, both in vacuum and CO2 atmosphere were carried out in compliance with proposed temperature profiles in Chapter 2.3.1. The target temperature ranges and temperature differences between the HI and CI were achieved, validating the system's ability to simulate space-like conditions.

However, inserting the hot copper plate (HCP) with connected copper belts (that are connected to left flange) into the TVAC damaged the connected sensor cables. This revealed a mechanical flaw in current setup and to enable safe and repeatable operation in future campaigns with cyclic thermal loads the preparation before testing must be executed differently.

While the thermal boundary tests with aluminium specimen were performed under controlled, steady-state conditions, unexpected variation in measured total resistance and thermal contact resistance were encountered, particularly tests with same input power (leading to similar heat flux measured).

The following factors were identified to be potential causes of the differences encountered:

- Formation of a curvature or radius of copper plates (HCP and CCP) at the interface with specimen during cooling, potentially reducing flat contact area with the aluminium specimen and leading to higher thermal contact resistance.
- Icing or condensation on the surface of the specimen during low-temperature testing (as described in Chapter 4.7). This can cause a transient thermal barrier between contact surfaces.
- Thermal expansion of the adhesive used for attaching thermocouples, which could spread to the interface between copper plate and aluminium specimen and change the contact resistance.
- Radiative heat transfer through microscopic gaps between the copper and aluminium surfaces, especially in vacuum. Even though radiation is usually small with respect to conduction, its relative influence increases when the contact is poor or discontinuous.
- Sensor drift or electronic instability, including changes in thermocouple behavior over time or after accumulated thermal cycles.
- Temperature influence on signal transmission, particularly in thermocouple wires and connectors. Temperature may also influence the analog voltage signals entering the ESAM data acquisition system and affect voltage-to-temperature conversion accuracy.

Even though it is not possible to estimate the contribution of each factor, their combination likely explains the observed variation in TCR values. The findings highlight the importance of rigid specimen mounting and sensor calibration in future thermal balance tests.

As a logical continuation of this work, the next step in testing will consist of measuring thermal contact resistance between aluminium plates. The setup will be modified by adding two aluminium plates, creating an aluminium-aluminium interface. This configuration will allow the isolation and investigation of thermal contact behavior specific to aluminium-aluminium contacts. Conducting these tests under the same boundary conditions as in thermal balance tests in this thesis will allow direct comparison with the previously tested aluminium-copper interface, providing further insight into the impact of material pairing on thermal resistance in vacuum.

# 8 Conclusion

This thesis focused on the experimental preparation, execution, and evaluation of thermal vacuum tests that would facilitate future calibration and qualification of a thermal vacuum chamber (TVAC) for testing the miniaturized heat switch (MHS). The primary goal was to ensure that the system would be able to simulate and measure space-relevant thermal conditions and contact effect accurately in vacuum and $CO_2$ atmospheres.

A combination of pilot, cyclic, and thermal balance tests were conducted to test major components of the TVAC system. Results confirmed that the test setup (involving heating, cooling and data acquisition) was able to provide controlled and reproducible temperature profiles. The conducted cyclic tests confirmed that both vacuum and $CO_2$ conditions were capable of achieving the desired temperature gradients and ranges, validating system operation readiness for more complex thermal loading conditions.

The use of specimens made of bronze and aluminium enabled systematic measurement of thermal parameters for a variety of interface conditions. While test procedure and temperature control were implemented successfully, difficulties were experienced in maintaining the consistency of thermal contact resistance measurement – namely in regulated thermal balance tests. These problems were traced to mechanical and thermal interface effects such as surface deformation, condensation, and thermal influence on adhesives and sensors. These effects are only hypothetical, and the actual cause must be clarified in further tests.

Despite these challenges, the methodology developed in this work (covering specimen insulation, temperature regulation, data verification, and post-processing using a thermal model) is a solid foundation for future development. The study also highlighted key areas that require improvement, including sensor cable protection during insertion of test stack and the significance of stable mechanical contact.

As a continuation of this study, future experiments will be carried out using a modified test stack configuration to evaluate the thermal contact resistance at an aluminium-aluminium interface. This will complement the methods developed in this thesis and allow direct comparison with the aluminium-copper results detailed here.

Overall, this thesis successfully prepared and demonstrated the test facility for future MHS component testing and made substantial contributions for the understanding of thermal interface behavior under different environmental conditions.

# 9 Bibliography


[1] ROTH, Alexander. *Vacuum technology*. 3rd, updated and enl. ed. Amsterdam: Elsevier, 1990. ISBN 04-448-8010-0.

[2] O'HANLON, John F. *A User's guide to vacuum technology*. 3rd ed. Hoboken: Wiley, 2003. ISBN 04-712-7052-0.

[3] *What Is Heat Transfer?* Online. 2024. Available: https://www.simscale.com/docs/simwiki/heat-transfer-thermal-analysis/what-is-heat-transfer/. [Accessed: 2025-05-19].

[4] BERGMAN, T. L. a INCROPERA, Frank P. *Fundamentals of heat and mass transfer*. 7th ed. Hoboken, NJ: Wiley, c2011. ISBN 978-047-0501-979.

[5] HOLMAN, J.P. *Heat Transfer*. 10th ed. New York: McGraw-Hill Education, 2010. ISBN 978–0–07–352936–3.

[6] *Heat Transfer*. Online. 2023. Available: https://www.engr.colostate.edu/CBE101/topics/heat_transfer.html. [Accessed: 2025-05-19].

[7] ÇENGEL, Yunus A. a GHAJAR, Afshin J. *HEAT AND MASS TRANSFER: FUNDAMENTALS & APPLICATIONS*. 5th ed. 2 Penn Plaza, New York, NY 10121: McGraw-Hill Education, 2015. ISBN 978-0-07-339818-1.

[8] EUROPEAN COOPERATION FOR SPACE STANDARDIZATION (ECSS). ECSS-Q-ST-70-04C, *Thermal testing for the evaluation of space materials, processes, mechanical parts and assemblies*. Second issue. 2008.

[9] EUROPEAN COOPERATION FOR SPACE STANDARDIZATION (ECSS). ECSS-E-HB-31-03A, *Thermal analysis handbook*. 2016.

[10] EUROPEAN COOPERATION FOR SPACE STANDARDIZATION. ECSS-Q-ST-70-02C, *Thermal vacuum outgassing test for the screening of space materials (ECSS)*. Second issue. 2008.

[11] NATIONAL AERONAUTICS AND SPACE ADMINISTRATION (NASA). GSFC-STD-7000A, *GENERAL ENVIRONMENTAL VERIFICATION STANDARD (GEVS) For GSFC Flight Programs and Projects*. Version A.

[12] LAZAR, Václav. *Calibration task of experimental device for space technology testing*. Master's thesis. Brno: Brno University of Technology, Faculty of Mechanical Engineering, Institute of Aerospace Engineering, 2019.

[13] LAZAR, Václav; MAŠEK, Jakub a HORÁK, Marek. *MHS - Design Evolution*. Brno, 2024.

[14] HUKSEFLUX THERMAL SENSORS. *USER MANUAL FHF02*. Online. 2006. Available: https://www.hukseflux.com/uploads/product-documents/FHF02_manual_v2006.pdf. [Accessed: 2025-05-08].

[15] *X60 – User Manual*. Online. Available: https://www.hbm.com/fileadmin/mediapool/hbmdoc/technical/A01650.pdf. [Accessed: 2025-05-15].

[16] *Signal Conditioner Amplifier System Traveller CF*. Online. 2012. Available: https://millp.co.in/wp-content/uploads/2018/10/Data-Sheet-Traveller-CF-2012-1.pdf. [Accessed: 2025-05-08].

[17] MAŠEK, Jakub. *Qualification Test of Heat Switch for Martian Conditions*. Master's thesis. Brno: Brno University of Technology, Faculty of Mechanical Engineering, Institute of Aerospace Engineering, 2016.

[18] LAZAR, Václav. *Advanced Analysis and Testing of Space Equipment Systems*. Doctoral thesis. Brno: Brno University of Technology, Faculty of Mechanical Engineering, Institute of Aerospace Engineering, 2024.

[19] GARDNER, Ethan L. W.; GARDNER, Julian W. a UDREA, Florin. Micromachined Thermal Gas Sensors—A Review. Online. *Sensors*. 2023, year. 23, č. 2. ISSN 1424-8220. Available: https://doi.org/10.3390/s23020681. [Accessed: 2025-03-22].

[20] *Edwards Vacuum 316L Stainless Steel Vacuum Ball Valves*. Online. Available: https://www.avantorsciences.com/in/en/product/38703869/edwards-vacuum-316l-stainless-steel-vacuum-ball-valves. [Accessed: 2025-05-08].

[21] *WRG- S - NW25 – Wide Range Gauge*. Online. Available: https://emea.my.edwardsvacuum.com/en/EUR/login. [Accessed: 2025-05-21].

# 10 List of Figures

# 11 List of Tables

# 12 Appendix

## A1-Photos of TVAC Systems/Subsystems & Equipment

*Figure 12.1 TVAC main body*

*Figure 12.2 Vacuum feedthrough [13]*

*Figure 12.3 Ball valve 1 & 2 [20]*


*Figure 12.4 Turbo-pumping station with TIC*

*Figure 12.5 Active wide range gauge [21]*

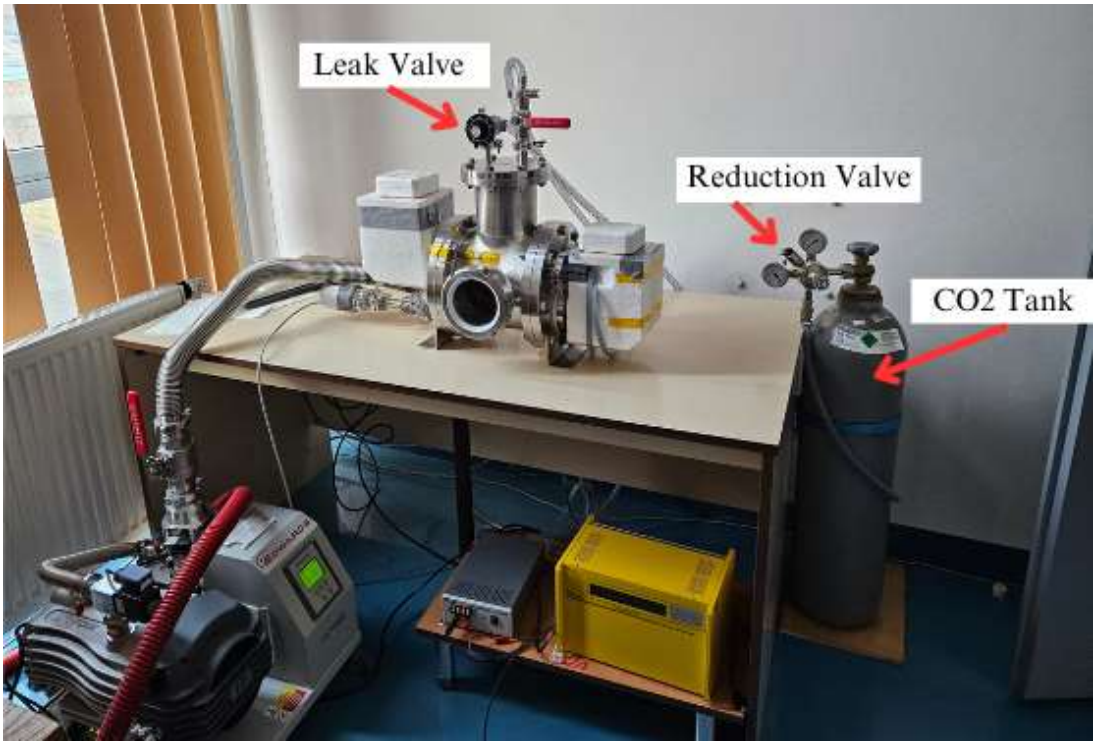


*Figure 12.6 $CO_2$ feed and regulation setup*

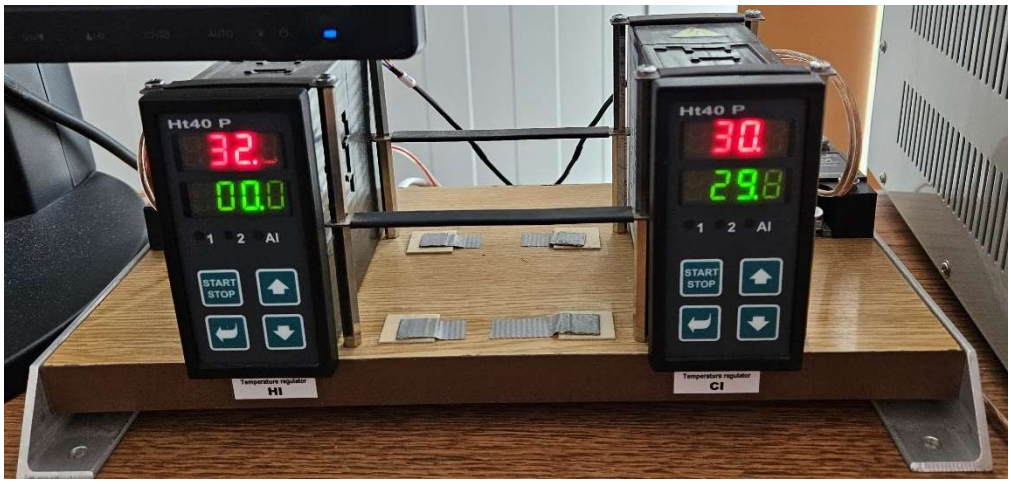


*Figure 12.7 PID regulators (HI regulator on the left, CI regulator on the right)*

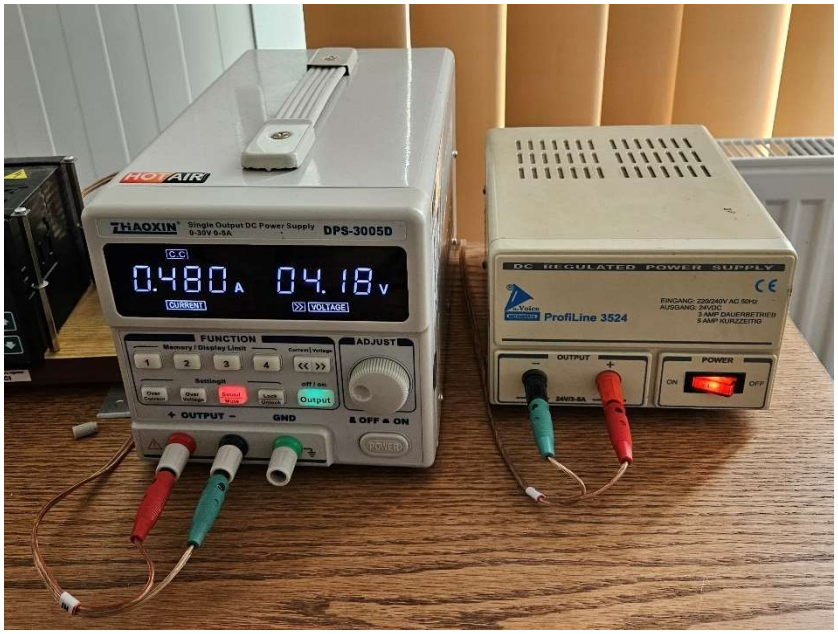


*Figure 12.8 HI power source (on the left) and CI power source (on the right)*

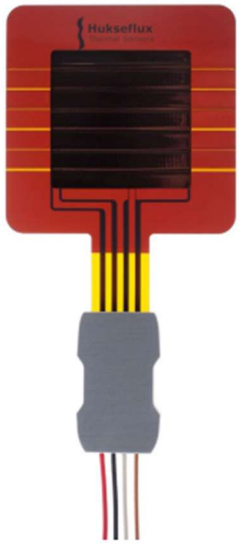


*Figure 12.9 FHF02 heat flux sensor [14]*

*Figure 12.10 Liquid nitrogen tank*


*Figure 12.11 ESAM Traveller with power source*

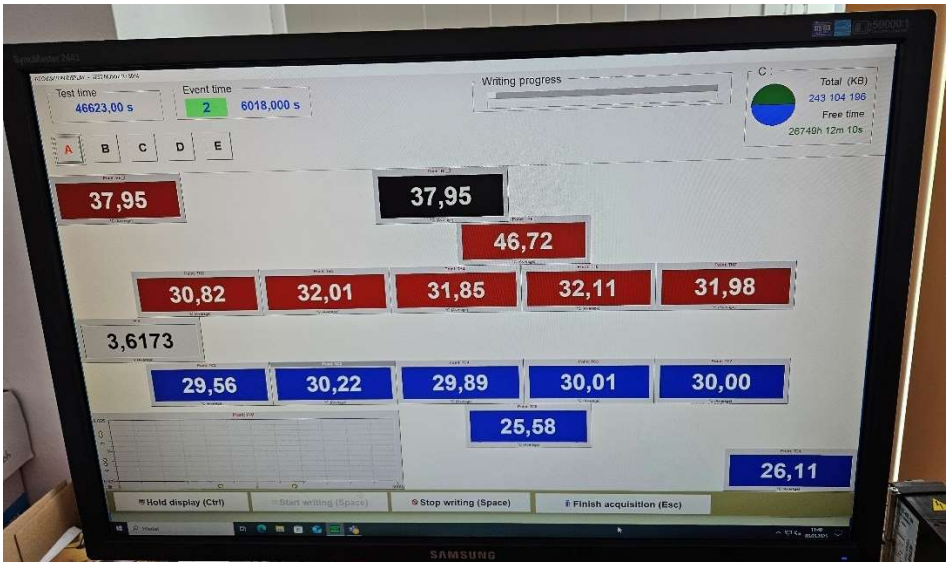


*Figure 12.12 ESAM software on PC*